energies

MDPI

Article

Grouped Charging of Decentralised Storage to Efficiently Control Collective Heating Systems: Limitations and Opportunities

Stef Jacobs [1,2,*] **, Margot De Pauw** [3,†] **, Senne Van Minnebruggen** [1] **, Sara Ghane** [4] **, Thomas Huybrechts** [4] **, Peter Hellinckx** [2] **and Ivan Verhaert** [1]

1   EMIB, Faculty of Applied Engineering, University of Antwerp, Groenenborgerlaan 171,
     2020 Antwerp, Belgium
2   Faculty of Applied Engineering–Electronics ICT, University of Antwerp, Groenenborgerlaan 171,
     2020 Antwerp, Belgium
3   Kenniscentrum Energie, Thomas More Kempen, Kleinhoefstraat 4, 2440 Geel, Belgium
4   IDLab, Faculty of Applied Engineering, University of Antwerp-imec, Sint-Pietersvliet 7,
     2000 Antwerp, Belgium
*   Correspondence: stef.jacobs@uantwerpen.be
†   Current address: Buildwise, Kleine Kloosterstraat 23, 1932 Zaventem, Belgium.

Abstract: Collective heating systems have multiple end-users with time-varying, often different temperature demands. There are several concepts catering to this, e.g., multi-pipe networks and 2-pipe networks with or without decentralised booster systems. In this study, we focus on 2-pipe networks with a changing supply temperature by smart use of decentralised storage. By grouping high-temperature demands, the average supply temperature can be lowered during large parts of the day, which is beneficial for system efficiency. The actual energy-saving potential, however, can be case-specific and is expected to depend on design choices and implemented control strategies. In this paper, these dependencies are assessed and identified by implementing two optimised rule-based control strategies, providing in such a way a bench-mark for other control strategies. The results show that grouping yields energy savings of up to 36% at similar peak demand as with conventional control strategies. The energy-saving potential is greatest for large storage volumes and small networks, but large networks with large storage and proper control choices can also achieve around 30% energy savings. Moreover, high-temperature time can easily be reduced to less than 40% of the day, which could make space cooling without decentralised booster heat pumps possible, but this requires further research.

Keywords: domestic hot water; DHW; decentralised storage; combined heat distribution; collective heating; temperature control; demand-based control; design impact

1. Introduction

District heating (DH) is a collective heating system that plays a key role in achieving the climate goals by 2050 [1–3]. Currently, DH only provides 9% of the total heat demand in Belgium, but according to the Horizon 2020 Heat Roadmap Europe projects, the cost-optimal share of DH by 2050 is 37% for Belgium [4] and perhaps 50% for Europe [5]. Collective heating systems are important for decarbonising heat supply because combining multiple end-users into one system leads to less fluctuating heat demands for central heat production units, which facilitates the integration of sustainable technologies, such as heat pumps (HP) [6]. The advantages of DH are also valid for collective systems at the level of apartment buildings [7].

There is a strong correlation between the overall efficiency of collective heating systems and the distribution temperatures [8,9]. The lower these are, the better the efficiency, due to lower distribution losses and better production efficiencies. In apartment buildings, gas

boilers or cogeneration are usually the heat sources for collective heating. Their efficiency strongly depends on the flow rate and return temperature. Due to the climate goals [1–3], there is now a shift towards the use of HP and electric boilers, whose coefficients of performance (COPs) depend strongly on the supply temperature [10] and indirectly on the return temperature. The benefits of reducing the central supply temperature in HP-based collective heating systems have been proved both in [11] for a space heating (SH) network and in [12] for a booster HP system producing domestic hot water (DHW) locally. However, when lowering the supply temperature, the limits to meet comfort requirements depend on the type of energy demand of end-users. SH can be supplied at both high temperatures (e.g., 75 °C with radiators) and low temperatures (ranging from 30 °C to 45 °C with, e.g., underfloor heating). The temperature of DHW at the tapping points needs to be 40 °C at least, but 55 °C is required to prevent *Legionella* growth [13]. If a heat exchanger is placed between distribution and offtake, an additional temperature difference is necessary for heat transfer. For these reasons, the main challenge for HP-based collective heating systems is to reduce the distribution temperatures as much as possible while still providing the required comfort to end-users.

When both low and high temperatures are produced centrally, a 4-pipe network usually provides heat distribution. In this research, however, we foresee a network in which all distribution occurs through only two pipes. Although decentralised booster HPs that locally raise the central temperature to the required temperature level [12,14] are a valid option for lowering distribution temperatures in 2-pipe systems, they have more refrigerant in the whole system, so they have a higher risk of leaks and a higher investment cost [15]. Therefore, the presented research proposes an alternative approach that can be applied within the context of an apartment building, i.e., the combined heating distribution circuit (CHDC), or within the context of a DH network.

When no booster systems are considered, the supply temperature set point ($T_{sup;SP}$) in 2-pipe systems is typically set to the hottest demand [16–18]. In a CHDC, the high-temperature demand is typically characterised by the DHW demand, whereas the space heating can be provided at a low temperature. However, according to studies [19,20], an end-user only consumes DHW for 1 to 3% of the day; thus, the fixed high $T_{sup;SP}$ seems unnecessary. For DH, this can be extended to buildings or end-users with an efficient low-temperature heat demand and buildings that require high-temperature heat. In both cases, high-temperature demand can be grouped for the central production units through smart use of decentralised storage (at the location) where high-temperature heat is needed and offers great potential to reduce supply temperatures during parts of the day.

All this points to the need for demand-based supply temperature control strategies that offer potential in HP-based collective heating systems with decentralised storage and different temperature-level requirements, but also that design has a major impact on unlocking their potential.

1.1. Present Control Strategies in Collective Heating

Currently, both data-oriented (e.g., [21,22]) and rule-based control strategies are the subject of ongoing research and are present in existing buildings. As our goal is to identify and understand potential savings, rule-based control strategies have the advantage of transparency compared to data-oriented solutions. Therefore, in this paper, we assess and optimise two rule-based control strategies and discuss the limitations and success factors. This will provide a benchmark for other control strategies, e.g., data-oriented ones.

The following studies focused on lowering the supply temperature of HP-based collective space heating systems where the DHW demand was neglected. Sun et al. [23] reduced the energy consumption of a building by 26.16% by variable control of the supply temperature of air-source HPs. Implementing rule-based adaptive supply temperature control in an office building resulted in energy savings of 38.2% [24]. The average supply temperature delivered by the central air-source HP was reduced by 8.4 °C. Verhelst et al. [25] optimised the operation of an air-to-water HP for the space heating of a single-family

building. Their optimisation led to cost savings of 5%. Luc et al. [26] identified the potential for flexible operation of DH network connected to a small district. To unlock the flexibility, the thermal mass of the buildings as the heat storage was used to shift the heat demand. In this respect, the indoor temperature set point was changed according to four scenarios, namely, three predefined time schedules and one based on dynamic price control for heat production. The results show that suitable control strategies can efficiently shift the load in a DH. Yang et al. [17] optimised the configuration of underfloor heating systems in the favour of DH. The thermal performance, energy flexibility, and economics were considered in the study for three DH scenarios (middle, low, and ultra-low temperatures). Again predefined schedules for the indoor temperature set point were used.

The operation of collective heating networks is also optimised when both SH and DHW demand are included. Benakopoulos et al. [27] presented a general overview of possible concepts for DHW production with low-temperature DH. Their focus was on the recirculation loop of 4-pipe systems in an apartment building (connected to a DH) rather than controlling the supply temperature of the centralised network (i.e., the DH). Three temperature-control strategies for CHDCs have been investigated by Vaillant Rebollar J. et al. [28], with a focus on controlling the recirculation flow rates in the central pipes to reduce the return temperature. In this respect, six configurations of the substations at the level of dwellings were considered: three variants with plate heat exchangers and three variants with decentralised DHW vessels. By using decentralised DHW vessels, the average return temperature could be lowered from 52 to 32 °C, and the distribution heat losses could be reduced by 10%. However, the recirculation control strategies were used for a CHDC with radiators (60 °C/40 °C regime), and the $T_{sup;SP}$ was always set to 62 °C. Therefore, the strategy to group the recharging of those vessels was not included in the analysis. In [29], it was reported that heat losses due to constant circulation of a DHW temperature of 58 °C accounted for 70.5% of the total energy demand of a CHDC without DHW vessels. In this study, temperature-control valves for controlling the bypass flow rate and a night setback of the supply temperature were tested in existing multifamily buildings. The temperature-control valves led to a 19.4% reduction in energy consumption compared to a fixed bypass flow rate, and reducing the supply temperature set point to 45 °C at night yielded energy savings of 13.2%. In [30], a tool for selecting the most suitable heating solutions by renovating apartment buildings was provided. Here, nine (collective) heating concepts are considered, where radiators or air heating systems were used to fulfil SH demands. One of the heating concepts considered was a CHDC with decentral DHW vessels and with the possibility of switching between high and low supply temperatures. In this respect, a charging time window (CTW) and electric resistance as a back-up heater in each DHW vessel were used. This concept had around 14% higher energy consumption than a 4-pipe system with a plate heat exchanger for DHW (and fixed supply temperature). However, the impacts of design choices and of control time settings on the system performance were not investigated. Therefore, their order of the best heating systems might change when optimal choices have been made.

Vanhoudt et al. [31] presented an active control strategy for heat delivery in a DH with central cogeneration of heat and power. The method is auction-based with the aim of shifting the cogeneration to times of high electricity price, so that larger profits can be made. To deliver flexibility to the production, different variants of central and decentralised thermal storage methods are considered, both in thermal storage vessels and in building mass. It was concluded that decentralised storage resulted in the highest profits for the cogeneration and system efficiency. In [32,33], new strategies for controlling the charging flow rate ($\dot{m}_{ch}$) of the central DHW storage tank were evaluated based on two temperature sensors in this tank, taking into account characteristics of the DHW demand. The studies were based on a DH that supplied a temperature of 80 °C, and the focus was on reducing the return temperature to the DH. The central DHW storage tank provides heat to a recirculation pipe in the apartment building. In [32], it was found that the locations of the temperature sensors had a larger influence on lowering the return temperature than controlling the

charging flow rate ($\dot{m}_{ch}$). Nonetheless, a lower $\dot{m}_{ch}$ reduced the return temperature by 5 to 8 °C. In [33], the control strategy of [32] was further optimised to lower the peak demand in the DH and lower the return temperatures by up to 16.4 °C. Additionally, other researchers stated that the design has a major impact on energy performances [34,35]. Lyu et al. [36] stated that the size of the central storage tank has a large influence on the efficiency of the central HP. Efkarpidis et al. [37] optimised the scheduling of recharging central storage with a focus on increasing the self consumption of solar panels and reducing the total energy cost. Again, a strong correlation between the potential of a certain control strategy and the sizing used was found.

It can be stated that the focus of research towards temperature-control strategies in collective heating systems does not include active temperature-control strategies that group high-temperature and low-temperature demands for the central production units. More specifically, decentralised storage is currently only used to provide flexibility to be able to control the amount of heat supply. Nevertheless, with the increase in HPs in collective heating networks, it is of great importance to reduce the supply temperature as often as possible, which can be achieved by switching between different temperatures.

1.2. Aim and Scope of the Paper

The focus of this research is on optimising the supply-temperature-control strategy for 2-pipe collective heating systems in apartment buildings. In the absence of appropriate supply-temperature-control strategies, the $T_{sup;SP}$ is usually fixed at the hottest demand, and decentralised storage is only used to reduce waiting times and to eliminate the need for bypass valves between supply and return [38]. In this respect, the contributions of the presented research are twofold:

1. A new method to control the supply temperature that groups the high-temperature and low-temperature demands in 2-pipe systems with decentralised storage is presented by means of two control strategies. First, a control strategy based on predefined time schedules, where the day is divided in times of high supply temperature to charge the vessels and times of low temperatures for SH. This approach is inspired by existing approaches for, e.g., electricity price (day/night tariffs) and schedules for indoor temperature set point schemes ([17,26]). The second control strategy is a novel approach based on two temperature sensors in each DHW vessel. The top sensor is for high-priority charging, and the bottom one is for low-priority charging.
2. By means of simulations, the presented supply-temperature-control strategies were assessed, and the impacts and optimisation limits of concept and design choices on potential performance were identified.

The conference paper [39] is a preliminary case study of this research showing that the potential is limited by design and control choices. In the current paper, the simulation framework is extended. More cases of collective heating network are included, allowing the effect of network size on the results to be evaluated. The research on design choices is further elaborated, considering sensor positions, central energy system designs, and storage insulation rates. This research has resulted in an elaborated discussion on the potential and boundary conditions of the suggested concept.

First of all, the scalable case study and control strategies for evaluating potential energy savings are described in Section 2. To this end, an assessment framework, described in Section 3, was used to efficiently investigate the influences of boundary conditions and design choices on the two control strategies in a simulation environment. A simulation-based approach is recommended by Vering et al. [10] because it considers the nonlinear inter-dependencies during operation, and because control and sizing influence each other. Furthermore, it also allows an objective evaluation by keeping the heat demand for DHW and SH the same for each design and control variant. By doing so, the optimisation limitations can be identified and generalised for the used key performance indicators (KPIs). The focuses of the KPIs are thermal comfort, primary energy (PE) consumption, and central peak power (CPP). Section 4 discusses the results of the different control and design

variants. The potential and main limitations of grouping same-temperature-level demands for demand-based supply-temperature-control strategies are discussed in Section 5, and Section 6 concludes this research.

2. Research Methodology

2.1. Case Description

The new supply temperature control methodology was assessed using simulations of CHDCs in apartment buildings in Belgium. The apartment buildings consist of identical dwellings occupied by different families of one to three residents. Each dwelling is connected to the CHDC and is equipped with a DHW vessel, which stores heat for one shower and two or three other tapping points, and underfloor heating with design temperatures of 35 °C/30 °C. All DHW vessels have a DHW priority switch, so the SH in a dwelling is switched off when its DHW vessel is thermally charged. The use of DHW vessels eliminates the need for hydraulic separations between CHDC and off-take, as the internal coil heat exchanger (CHE) in the vessels separates the DHW from the technical water in the CHDC, and no bypass is needed in the CHDC. Passive mixing in any underfloor heating system is used to distribute a maximum of 35 °C through the floor pipes, even if higher temperatures are distributed in the CHDC. The indoor temperature set point is 21 °C during the day and 19 °C at night, for a design heat load of 1340 W at –8 °C outside.

The central energy system consists of a geothermal heat pump (GHP) connected to central storage and a high-temperature unit (HT-unit). This unit is needed to raise the supply temperature to 65 °C when required by the control strategy. Since this HT-unit has a significant impact on energy consumption, different set-ups were investigated, namely, a gas boiler, an electric boiler (e-boiler), and a high-temperature HP (HT-HP). Figure 1 gives a schematic overview of the case.
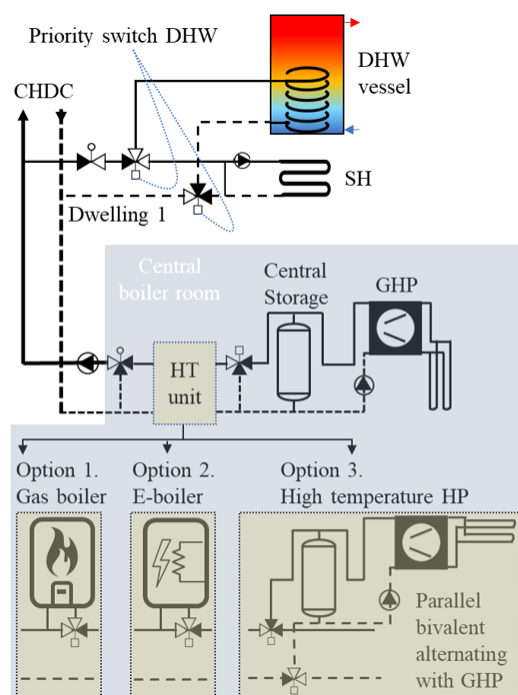
Figure 1. Overview of the case study. Each dwelling is equipped with underfloor heating and a domestic hot water (DHW) vessel. The central production consists of a geothermal heat pump (GHP) and an high-temperature-unit (HT-unit, i.e., gas boiler, e-boiler, or high-temperature heat pump (HT-HP)).

The GHP was sized to cover the SH demand, i.e., 29 kW. The central storage tank had one temperature sensor at the top and one at the bottom of the tank, both with a set point of 45 °C. The HT-units were sized to cover the DHW peak demand. For a gas

boiler and GHP, a series connection is preferable. Although a parallel connection leads to a lower inlet temperature for the gas boiler, it only leads to negligible efficiency gains if the boiler's two-way valve is controlled with complex modulation [36]. The inlet temperature of the e-boiler should be as high as possible, and therefore is in series with the GHP. When an HT-HP is considered, the connection to the GHP is parallel, and bivalent-alternating. The HT-HP only operates to deliver 65 °C, starting from the return temperature of the CHDC. It is connected to a second storage system for stable operation.

2.2. Mathematical Estimation of Optimisation Potential

The demand-based control strategies should supply both low (i.e., 38 °C for SH with underfloor heating) and high (i.e., 65° for charging DHW vessels) temperatures. A straightforward control strategy is to raise the supply temperature each time one of the DHW vessels needs to be charged according to their temperature sensor. Although the temperature can be lowered outside these charging cycles, preliminary results showed that low supply temperatures rarely occur for such a basic control strategy (only PE savings of up to 3% possible). These minor PE savings are probably the reason why such current systems are still controlled with a fixed supply temperature. Hence, the optimisation methodology of this paper is to group the charging of decentralised DHW vessels and use their thermal inertia to supply a low temperature during the other parts of the day. In this way, the aim is to reduce heat losses and increase production efficiency, resulting in primary energy (PE) savings. Through the following hypothesis, the energy savings of grouped recharging were estimated for an apartment building of 20 dwellings.

As mentioned in Section 2.1, each of the 20 dwellings has a design heat load of 1340 W, consisting of transmission and ventilation losses. The average outdoor temperature in Belgium during January is 3 °C [40], leading to an average daily space heating demand of 20 kWh/day per dwelling. The heating power of underfloor heating is 25 W/m² on average, and the floor area for our apartments is 100 m²; thus, the heating was switched on for 8 h a day in each dwelling. The average daily DHW demand is 4 kWh/day per dwelling in a European apartment building [20]. Considering a DHW vessel of 90 L with a set point of 58 °C and a stratification efficiency of 70%, the useful energy in the storage vessel is 3.5 kWh. The internal CHE of the DHW vessels in the Belgian case study has a UA-value of 500 W/K and design temperatures of 65 °C/50 °C, resulting in a heating power of 7.1 kW. Therefore, recharging of a particular DHW vessel occurs for 0.56 h a day.

The distribution losses are based on the required recharging times for DHW vessels and the distribution temperature. In the case of the reference control, the 20 DHW vessels might be recharged separately (20 × 0.56 h), and SH might be used during the other 8 h, meaning a total heating time of 19.2 h. In the case of optimised control, the recharging of DHW vessels is fully grouped and SH is provided at low distribution temperatures. Therefore, the high-temperature head would be needed for only 0.56 h and the low temperature for 8 h. The stainless steel water pipes were dimensioned at DN65 and had a total length of 120 m to deliver the heat at a maximum water velocity of 1 m/s. The piping heat transfer was 0.265 W/mK per meter according to Equation (1), with EPS insulation (λ_{EPS}) [41]. Therefore, the reference control causes heat losses of 44.4 kWh/day at 65 °C/50 °C, and the controller that charges in groups loses only 2.5 kWh/day at 65 °C/50 °C and 18.2 kWh/day at 35 °C/30 °C. A total reduction in distribution losses of 56.9% is possible.

$$U_{pipe;m} = \frac{1}{2\pi}\left[\frac{1}{\lambda_1 r_1} + \frac{ln\left(\frac{r_2}{r_1}\right)}{\lambda_{steel}} + \frac{ln\left(\frac{r_3}{r_2}\right)}{\lambda_{EPS}} + \frac{1}{\lambda_3 r_3}\right] \tag{1}$$

Here λ_1 is the conductivity between water and the pipe in relation to the water's velocity [41], r_1 is the inner pipe radius (32.5 mm), r_2 is the outer pipe radius (36.5 mm), r_3 is the radius up to the insulation surface (71.5 mm), λ_{steel} is the conductivity of steel [41], and λ_3 is 8 W/m²K.

The set point of the central storage is 45 °C; thus, the GHP delivers all heat up to 45 °C. The average return temperature is 33 °C concerning the share of heat demands. Therefore, the GHP's COP is 5 on average, based on the used GHP model described in Section 3.1.5. The factor to convert electricity to PE is 2.5 in Belgium [42]. The central boiler has an efficiency of 100%, as this is the most beneficial for reference control. To deliver the demanded heat and compensate for the distribution losses, the total PE consumption for the reference control strategy (all demand supplied at 65 °C) would be 428.8 kWh/day, while grouped charging of DHW vessels would require only 275.3 kWh/day. In conclusion, the estimated PE savings by grouping the charging cycles of all 20 decentralised 90 L DHW vessels is 35.8% in January.

2.3. Strategies for Grouped Charging of DHW Vessels and Sensitivity Analyses

In order to translate the new grouped charging methodology into implementable control strategies, two options are proposed and investigated in this research. Figure 2 shows (a) the reference control (REF-control), and in (b) and (c) are the two new control strategies of this research. The first one (Figure 2b) divides the day into times of high temperature and times of low temperature based on pre-defined charging time windows (CTWs). This is similar to a day and night tariff structure for electricity, but now for recharging the decentralised DHW storage vessels. The second one (Figure 2c) is a more innovative control approach, which is based on two sensors in each DHW vessel, with the upper sensor (T2) serving high-priority charging and the lower one (T1) serving low-priority charging.
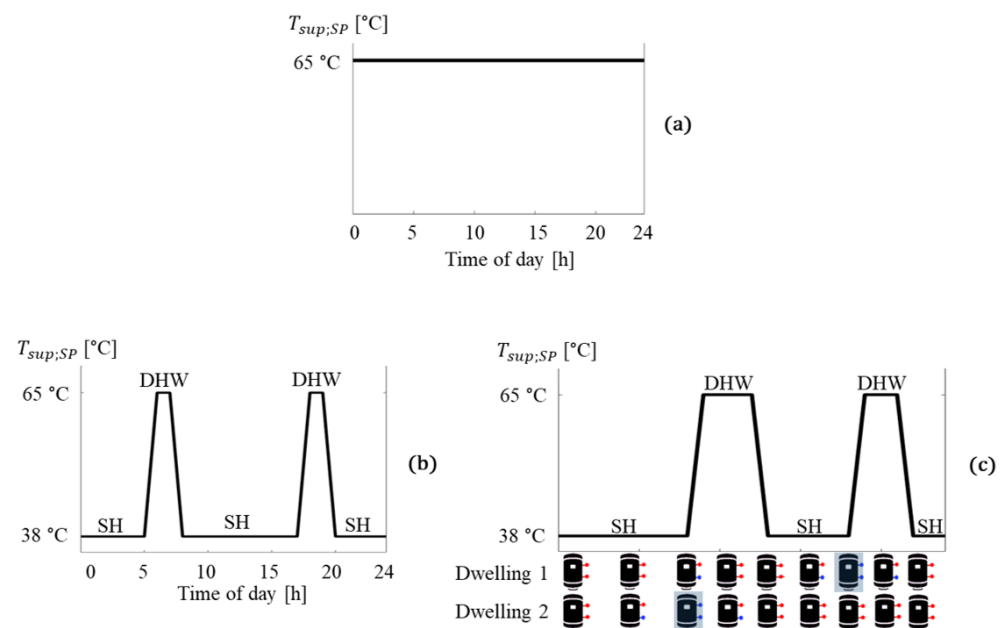

Figure 2. The three supply-temperature-control strategies used are (**a**) reference control, (**b**) time-based control (TB-control), and (**c**) two-sensor control (2SC). For TB-control, $T_{sup;SP}$ is 65 °C during two pre-defined charging time windows (CTWs) and 38 °C otherwise. A DHW vessel stops recharging during a CTW once the bottom sensor reaches the DHW set point. For 2SC, each DHW vessel has two temperature sensors. The $T_{sup;SP}$ is 65 °C when the upper sensor (T2) of one of the DHW vessels drops below the DHW set point. Then, all DHW vessels with a too-cold lower sensor (T1) are recharged. As soon as the temperature of the lower sensor of all DHW vessels rises above the set point, the central supply temperature drops back to 38 °C.

2.3.1. Reference Control Strategy (REF-Control)

The REF-control was a constant high $T_{sup;SP}$ of 65 °C both for SH and DHW demands, as shown in Figure 2a. The DHW vessels had one sensor at 2/3 height and a set point of 58 °C with an on/off control hysteresis of ±3 °C. The $\dot{m}_{ch}$ of the DHW vessels was originally

600 kg/h. For this REF-control, the impacts of the larger storage volumes (150 L and 200 L) and smaller $\dot{m}_{ch}$ (500 kg/h to 100 kg/h) on system performance were briefly investigated.

2.3.2. Time-Based Control Strategy (TB-Control)

An example of the time-based control (TB-control) with two pre-defined CTWs for raising the $T_{sup;SP}$ to 65 °C is shown in Figure 2b. All DHW vessels, with demand according to one temperature sensor at the bottom of the vessel (i.e., $T < 58\,°C − 3\,°C$), are thermally recharged during the high-temperature CTWs until the sensors' temperatures exceed 61 °C. The CTW needs to be tailored to the DHW consumption pattern of end-users in the building, which makes this control strategy sensitive to time settings. The optimal high-temperature start times must be determined for each building case. For this research case, the CTW start times are on average 30 min before the largest increase in DHW demand for the entire building, i.e., 7:00 and 17:00, so that vessels start charging on time and higher heating capacity is available when DHW demand is high. The storage volume and CTW length are important to ensure DHW comfort during periods of low supply temperature, but the larger these parameters, the higher the energy consumption. Moreover, $\dot{m}_{ch}$ affects CPP and DHW comfort. Sensitivity analyses were therefore carried out for these three design choices. The volume of an individual DHW vessel was varied among 90 L, 150 L, 200 L, and 300 L. The volume was increased to 300 L, as preliminary results have already shown that 90 L vessels do not provide sufficient DHW in most CTWs. The length of the CTW was increased from $2 × 0.5$ h to $2 × 2$ h, in 30 min increments, and then to $2 × 3$ h. The $\dot{m}_{ch}$ was set to 600, 300, or 100 kg/h. This sums up to a total of 60 design variants for the TB-control strategy (i.e., 4 volumes, 5 CTWs, and 3 different $\dot{m}_{ch}$).

2.3.3. Two-Sensor Control Strategy (2SC)

A generalisable control strategy is the sensor-based control strategy that uses two temperature sensors in each DHW vessel for grouped charging (see Figure 2c). The upper sensor (T2) is intended for high-priority charging of the respective DHW vessel and can initiate high central supply temperatures. The lower sensor (T1) starts charging the respective DHW vessel only when the central supply temperature is already high. In this way, vessels that are slightly thermally discharged are not charged immediately, but only when there are also fully discharged DHW vessels in the CHDC (when T2 is too cold). Specifically, when one of the T2 sensors in any DHW vessel gives a reloading signal ($T < 58\,°C − $ hysteresis), the central $T_{sup;SP}$ is raised from 38 to 65 °C, and all vessels with demands according to their lower sensors (T1) are loaded simultaneously. Once the T1 sensor in each DHW vessel is satisfied (T > 58 °C + hysteresis), the central temperature set point is set back to 38 °C. The advantage of using the two sensors is that the typical average DHW consumption pattern does not need to be known in advance for any control setting.

Again, the $\dot{m}_{ch}$ (from 600 to 100 kg/h) and the volume of an individual DHW vessel (90, 150, and 200 L) were varied. In addition, the positions of those two sensors and the hysteresis were analysed. Both the position and the hysteresis around the set point for DHW (58 °C) have an influence on when the supply temperature is increased to 65 °C and when it is dropped to 38 °C. The two sensors their positions were only varied for a $\dot{m}_{ch}$ of 600 kg/h for each volume. The larger the storage volume, the more sensor positions are available. Six combinations of sensor positions for 90 L and nine for both 150 L and 200 L were considered. Then, for each of the 3 volumes, the combination of sensor positions with the best trade-off between DHW comfort, energy consumption, and central peak power was selected (see Section 4.3.1). These positions were used for analysing the effects of 3 hystereses (3 °C, 4 °C and 5 °C) and of 6 different $\dot{m}_{ch}$ (600 to 100 kg/h). A total of 78 variants of the 2SC strategy were analysed.

2.3.4. Additional Analyses

Representative variants from each control strategy were subjected to four additional analyses to generalise the results. First, the number of dwellings was varied (30, 20,

10, or 6 dwellings) to assess the dependence on the size of apartment buildings, which affects the potential to group charging times. Next, the insulation level of the DHW vessels was varied (Ecodesign labels: "A+", "C", and "F"), as this impacts the optimal storage volume and recharging frequency due to increased heat losses. Third, different types of high-temperature units in the energy system were investigated (see Section 2.1). Finally, the results of the idealised approach were verified with a non-idealised central energy system to test the influence of time delays in the production units. In the non-idealised case, the HT-unit is a gas boiler. A total of 21 variants were selected, which meant 168 additional one-month simulations (i.e., 3 additional numbers of dwellings, 2 additional vessel insulation rates, 2 other HT-units, and 1 non-idealised energy system for 21 variants) were performed, as the previous analyses already covered 20 dwellings and "A+" insulated vessels.

3. Assessment Framework

A dynamic simulation environment was built in Matlab to assess control strategies and study the effects of different design choices. All models were solved with a step size (Δt) of 10 s to simulate the DHW use in detail. The verification of the simulation environment was done by checking energy balances for every single time step. The maximal error of the various energy balances was less than 0.00001 joule.

3.1. Simulation Environment

The models were based on the doctoral dissertation of Van Riet [43]. This environment represents the dynamic thermal behaviour of the CHDC and its components. The transient behaviour is considered by first order, ordinary, linear, and non-homogeneous differential equations according to the general equation described in [7] and as in the IDEAS library [44] for simulating district heating networks. Due to the Δt of 10 s and the used simulation models, the simulation period was fixed to one month to reduce the computational time and power. The month of January was selected, as here the SH demand is larger than in spring or autumn; thus, it best shows the impact of the proposed methodology. The most important models are briefly described, and the used KPIs are discussed.

3.1.1. Demand Profiles

The internal heat gains ($\dot{Q}_{int}$), occupancy profiles, and DHW demand profiles were based on a stochastic "profile generator" developed in the TETRA-SWW [45] and Install2020 [46] projects. The generator was based on statistical occupancy data of different family types in Belgium. These different profiles of a particular dwelling are also linked to each other, so that, for example, there is only a DHW demand in a particular dwelling when someone is present. An example of the cumulative DHW demand at 60 °C for six families is given in Figure 3a. The occupancy profiles for the same families are shown in Figure 3b. For readability, only two days in January and 6 out of 20 families are shown. As can be noticed, the profiles are different for each dwelling and throughout the year. In each dwelling, the indoor temperature set points are coupled to the respective occupancy profiles.

3.1.2. Dwelling Thermal Model

By electrical analogy, each dwelling was represented by a 3R2C model, as shown in Figure 4. Each dwelling was a single thermal zone without heat transfer to neighbouring dwellings and consisted of two heat capacities, namely, the zone (C_z) and walls (C_w) (J/K). C_w was calculated according to medium-heavy walls [42], and C_z was five times the heat capacity of the indoor air volume, V_z in (m³), to take account of the furniture.
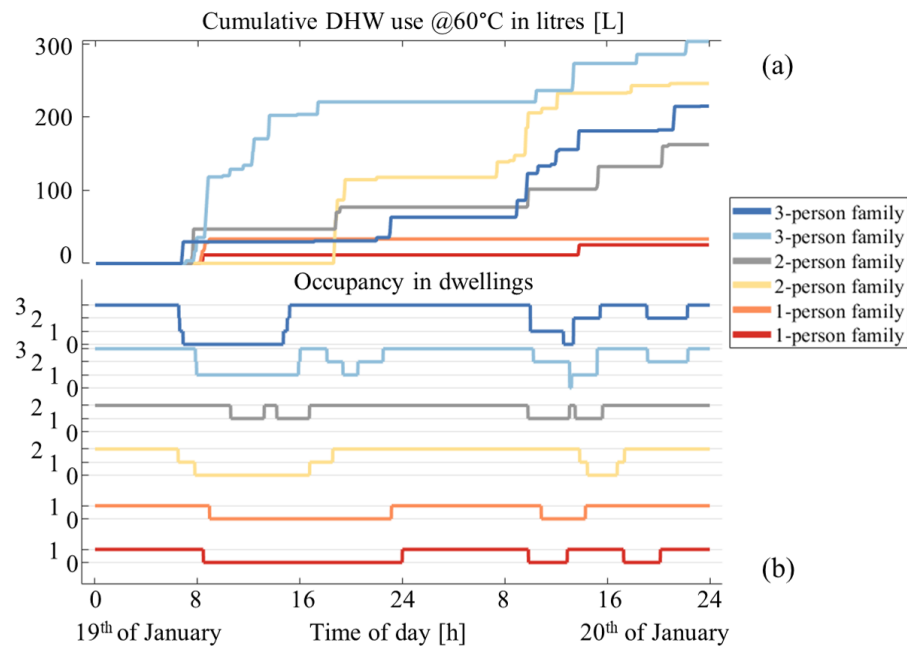
Figure 3. Example of a DHW profile (**a**) and occupancy profile (**b**) for six different families. The profiles are given for the 19th and 20th of January.

The three heat flows, $\dot{Q}_{em;tot}$, $\dot{Q}_{int}$, and $\dot{Q}_{sol}$ (all in W), were transferred to both the zone and walls. In order to simulate $\dot{Q}_{em;tot}$, the underfloor heating was segmented in three equal parts with a uniform temperature, as was done in [43]. The thermal capacity of the underfloor heating was 15.12 MJ/K. The outdoor temperature (T_{ext}) and solar radiation ($\dot{Q}_{sol}$) were based on weather data from Belgium [47]. The model consists of three temperature nodes (°C), namely, the outdoor temperature (T_{ext}); the temperature of indoor air and furniture (T_z); and the temperature of the walls, floor, and ceiling (T_w). Between each node is an overall heat transfer coefficient (UA), in order to quantify the resistance of heat exchange. The following two differential equations describe the behaviour of T_z and T_w. These equations were drawn from the 3R2C model in Figure 4.

$$
\begin{aligned}
C_z \frac{dT_z}{dt} = &(1 - 0.5r_{em})\,\dot{Q}_{em,tot} + (1 - 0.5r_{sol})\,\dot{Q}_{sol} + (1 - 0.5r_{int})\,\dot{Q}_{int} \\
&- UA_{z,w} \cdot (T_z - T_w) \\
&- c_{p,air} \cdot \dot{m}_v \cdot (T_z - T_{ext})
\end{aligned}
\tag{2}
$$

$$
\begin{aligned}
C_w \frac{dT_w}{dt} = &(0.5r_{em})\,\dot{Q}_{em,tot} + (0.5r_{sol})\,\dot{Q}_{sol} + (0.5r_{int})\,\dot{Q}_{int} \\
&+ UA_{z,w} \cdot (T_z - T_w) \\
&- UA_{w,ext} \cdot (T_w - T_{ext})
\end{aligned}
\tag{3}
$$

Here r_{em}, r_{sol}, and r_{int} are the proportions of radiant heat from the emitter, which for underfloor heating was taken to be 50%; for solar radiation gains, 100%; and for internal heat gains, 50%. Of the radiant heat, 50% is transferred to T_w and 50% to T_z, since the zone node also includes the furniture in the zone. The other proportion is transmitted through convection. In Equation (2), T_w is from the previous time step, and T_z in Equation (3) is calculated in Equation (2). The ventilation flow rate $\dot{m}_v$ equals $\frac{1}{3600} \cdot \rho_{air} \cdot n_{v;tot} \cdot V_z$, and $n_{v;tot}$ is the ventilation rate per hour of the indoor air based on hygienic minimums.
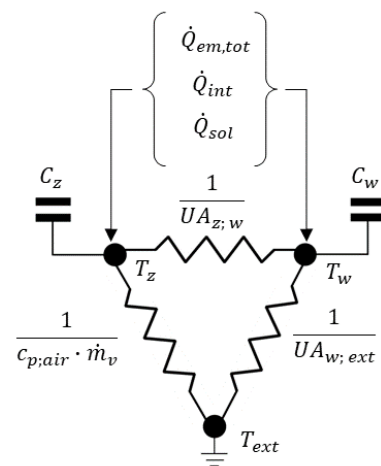
Figure 4. The 3R2C model of one dwelling in the apartment building. The temperature is calculated for a node in the indoor air (T_z) and in the wall (T_w). The outdoor temperature (T_{ext}) is derived from a weather profile in Belgium [47]. The heat flow from solar gains ($\dot{Q}_{sol}$), indoor heat gains ($\dot{Q}_{int}$), and the underfloor heating ($\dot{Q}_{em}$) are divided over the zone and wall node.

3.1.3. DHW Vessel Model

The stratified storage tank model was simulated as a partial differential equation both in temperature and height. In the model, each DHW vessel has an internal CHE in the lower half of the vessel and two ports at 0% and 100% of the height. The model is based on Type 60 of TRNSYS [48] and is described in [43]. The stratified vessel is divided into several homogeneous water layers of about 20 L (depending on total volume; e.g., 90 L has 4 layers of 22.5 L). Heat transfer to the adjacent layers by conduction and advection is taken into account, along with losses to the environment and heat gains from the internal CHE. A temperature-inverse algorithm was added to account for the effect of temperature on the density of water. At the inlet and outlet, conduction and the heat losses through the top and bottom surfaces are neglected. The sizing (UA-value (W/K)) of the internal CHE was fitted to laboratory measurements of a 90 L vessel and technical information from Collindi [49]. The heating capacity of the CHE increases in larger DHW vessels, as more place is available for the CHE. Thus, more heating power is available to heat a larger DHW vessel. Therefore, the UA-value of the CHE is multiplied by a correction factor ($f_{CHE;vol}$), based on recommendations of [49] and shown in Table 1. The UA-value of the CHE is not adjusted for $\dot{m}_{ch}$, which means that it is narrower and longer at smaller charging flow rates.

Table 1. Correction factor for sizing the internal coil heat exchanger of the DHW vessel.

Volume of DHW Vessel	$f_{CHE;vol}$
90 L	1
150 L	11/9
200 L	12/9
300 L	14/9

3.1.4. Hydraulic Models

The hydraulic models of the control valves and pumps were simplified to reduce model complexity and decrease calculation time. More specifically, control signals adjust the flow rate directly, without depending on hydraulic models and hydraulic dependencies [50]. This means that the mass flow between the nominal value and 10% of this value is guaranteed to be available. Time delays of control valves are taken into account with a time constant (τ) of 32 s, as in [43]. The time delay in the pipes is modelled by applying the plug-flow principle [51].

3.1.5. Central Energy System Models: GHP and Boiler

For most of the simulations, the energy system is considered ideal; thus, it can instantaneously deliver the demanded supply temperature and flow rate. This approach was chosen because it allows focusing on the evaluation of control strategies, without considering the effects of transient behaviour in production units, their sizing, and the behaviour of PID controllers. The results of the most representative variants of all control strategies were also validated in a non-idealised central energy system, consisting of the GHP and a gas boiler in series, to quantify the PE savings when time delays in the production room exist.

For the idealised approach, the temperature at the start of the CHDC's supply pipe equals the imposed temperature set point of the control strategy, i.e., $T_{sup;SP}$. Afterwards, in the post-processing, the coefficient of performance (COP) of the GHP, its electricity use, and the additional energy consumption of the HT-unit are calculated. The source temperature of the GHP was set to 10 °C. The COP_{des} is four at B10/W55 according to Viesmann [52] and was adjusted according to the EPB calculation method [42]. Equation (4) shows this adjustment to the GHP's design outlet temperature—T_{out}, equal to 45 °C—and to the inlet temperature (T_{in} [°C]), namely, the CHDC's return temperature (T_{ret}). If $T_{sup;SP}$ is above 45 °C, extra heat is provided by the HT-unit. In case of a gas boiler or e-boiler, the HT-unit's efficiency is 100%. This efficiency was chosen because it is the most advantageous for a constantly high supply temperature, and therefore is the most stringent for the alternative control strategies. In the case of a high-temperature HP as the HT-unit, the COP of the HT-HP is also calculated as in Equation (4), but with T_{out} being equal to 65 °C, and T_{ret}, coming from the GHP, is then 45 °C.

$$COP = COP_{des} \cdot (1 + 0.02 \cdot (55 - T_{out})) \cdot (1 + 0.01 \cdot ((T_{out} - T_{in}) - 8)) \tag{4}$$

The energy consumed per time step (Δt) by the idealised central energy system is based on the demanded mass flow in the CHDC ($\dot{m}_{CHDC}$ (kg/s)) and the distribution temperatures ($T_{sup;SP}$ and T_{ret} [°C]). Equation (5) calculates the electricity consumed by the GHP with $T_{in} = T_{ret}$; and the additional energy consumed by the HT-unit, when $T_{sup;SP} > 45$ °C, is discovered according to Equation (6), with $T_{in} = 45$ °C. Only for the HT-HP was the calculated consumed energy of Equation (5) divided by the HT-HP's COP.

$$P_{HP} = \frac{\dot{m}_{CHDC} \cdot 4187 \, \frac{J}{kgK} \cdot max[0 \, °C, (min(T_{sup;SP}, \, 45 \, °C) - T_{in})]}{COP} \cdot \Delta t \tag{5}$$

$$P_{boi} = \dot{m}_{CHDC} \cdot 4187 \, \frac{J}{kgK} \cdot max[0 \, °C, (T_{sup;SP} - T_{in})] \cdot \Delta t \tag{6}$$

In the non-idealised approach for the last analysis, the models of the GHP and the gas boiler are based on performance maps derived from measurements and manufacturers. The generalised ordinary differential equation is given in Equation (7), with C^{prd} being the thermal capacity of the production unit (J/K) at temperature T_{out} (°C); $\dot{Q}_{prd}$ the source heat of the production unit, based on thermal efficiency (W); UA_{prd} the overall heat transfer coefficient (W/K) to the surroundings (at 20 °C); and $\dot{m}_{prd}$ the flow rate passing through the production unit (kg/s), entering at an temperature T_{in} (°C). The central storage tank is similar to the model of DHW vessels, but without an internal CHE and with two temperature sensors (one at the top and one at the bottom).

$$C_{prd} \frac{dT_{out}}{dt} = \dot{Q}_{prd} - UA_{prd} \cdot (T_{out} - 20 \, °C) - \dot{m}_{prd} \cdot 4187 \, \frac{J}{kgK} \cdot (T_{out} - T_{in}) \tag{7}$$

To size the central energy system, the new sizing method for CHDCs [53] was used, which was recently validated in [54]. The sizing method gives all possible combinations of thermal power in kW and "active" storage capacity in kWh to meet the peak heat demand. It might be possible to consider the storage capacity of the decentral DHW vessels as central

storage capacity, making it possible to reduce the required thermal production power. However, this approach has not yet been validated. Therefore, the required thermal power of the central production for a 20-unit apartment building is 110 kW. The GHP was sized to cover the peak heat demand of SH (29 kW), and the boiler was sized to meet the additional power required for DHW (110 kW – 29 kW = 81 kW). The central storage, connected to the GHP, was sized to store the heat produced in one hour by the GHP at design temperatures of 45 °C/35 °C.

3.2. Key Performance Indicators (KPIs)

The KPIs used in this research reflect the impacts of the control strategies on energy efficiency, on required sizing of the CHDC, and on thermal comfort provided to end-users.

In terms of energy efficiency, four KPIs were used. The first was the total primary energy (PE) use of the system (PE_{use} (kWh)) relative to the PE_{use} of the reference control strategy with reference design parameters, i.e., ($PE_{use}/PE_{use;ref}$) × 100, denoted by $\%_{PE}$ (%). The design parameters were set according to the case study in Belgium: the reference volume was 90 L with an $\dot{m}_{ch}$ of 600 kg/h. The energy use of the GHP (electricity) and gas boiler (fossil fuel), e-boiler (electricity) or high-temperature HP (electricity) were calculated as described in Section 3.1.5 with respect to the type of central energy system. The conversion factor for electricity to PE was 2.5 in Belgium [55]. This KPI is important, since this research aims at reducing the total energy use. It should be noted that using the same reference for each variant also makes it possible to compare variants and thus calculate energy savings between variants. The second is the primary energy ratio (PER). This is the total efficiency in terms of PE, i.e., the ratio of the useful PE to PE_{use}. The useful PE consists of the consumed energy for both SH and DHW. A higher PER indicates a higher GHP share in heat supply and lower heat losses. The third was the average return temperature ($\bar{T}_{ret}$ (°C)) at the central energy system level (i.e., the temperature entering the energy system). Finally, the $\%T_{high}$ (%) was used, which represents the time the central supply temperature is above 50 °C, when there is mass flow in the distribution pipe, relative to the total simulated period (one month). $\bar{T}_{ret}$ and $\%T_{high}$ give more insight on why a certain control or design choice influences the energy efficiency.

The central peak power (CPP) (kW) quantifies the impact on sizing. This is the most power delivered by the central energy system over a period of 10 min. This time frame is selected to have more realistic values for an ideal production, since it provides unrealistic temperature increases without considering thermal inertia. The lower this CPP, the high-temperature unit and distribution pipes can be made smaller, which reduces investment costs. Moreover, a reduction in CPP increases overall energy performance, as production units are more likely to operate close to the full load.

To represent the DHW comfort, the relative duration of lacking DHW temperature ($t_{DHW;dc}$) (%) is introduced as a KPI. This is the proportion of the total tapping time of all vessels in which the DHW temperature is lower than 40 °C. Figure 5 illustrates this KPI with an example. This graph represents the mean of all tapping periods of one vessel. The top temperature in the vessels (in red) is the temperature used for DHW (the set point is 58 °C). The orange, light blue, and dark blue lines are temperatures in other layers of the vessel. An ideal mixing valve after the DHW vessel is assumed to regulate the mass flows towards a consumption temperature of 40 °C. A top temperature below 40 °C is considered as DHW discomfort. The total discomfort time is A, and the total tapping time is B; thus, the relative duration of DHW discomfort is A/B, given as a percentage. In contrast to a temperature lack that occurs at the beginning of a tapping, which is related to pipe lengths, this discomfort is solely due to sizing or late recharging of vessels. The smaller this percentage, the less time the end-users experience discomfort on average. The distribution pipes from the vessel to the tapping points are not evaluated.

Finally, the room temperature lack (RTL) (Kh/day), as in [43], is used as a metric to quantify the average indoor thermal comfort of the dwelling. For each dwelling, the av-

erage number of Kh per day used when the indoor air temperature is below the indoor temperature's set point is calculated.
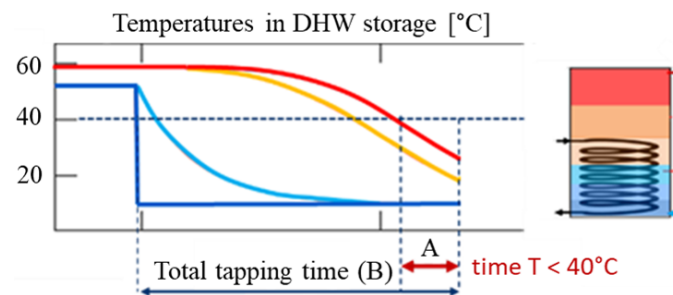

Figure 5. Example of DHW discomfort duration key performance indicator (KPI). The colours refer to the temperature layers of the DHW vessels. This KPI is calculated as A/B, where B is the total tapping time of all end-users and A is the total time at which the DHW temperature is below 40 °C.

4. Results

This section discusses the influence of different design variants on control strategies that group the same-temperature-level demands—first by control strategy, and then the additional analyses of most representative variants. In most graphs, the shape refers to the volume of the DHW vessel, the colour to the $\dot{m}_{ch}$, and the darkness of the colour to the level of hysteresis used (for 2SC only), unless otherwise stated.

4.1. Design's Influences on REF-Control

Before analysing the control strategies for grouped charging, the effects of storage volume and charging flow rates on REF-control performance were briefly examined (see also [39]). It was found that increasing the DHW vessel volume increases the comfort for both DHW and SH, while having no significant impact on PE_{use}. The main reason for this improved DHW comfort with similar PE_{use} for larger vessels is the high insulation rate of the DHW vessels (Ecodesign label "A+"). Larger vessels indeed have higher permanent heat losses (the losses of 90 L were around 80% of those of 200 L vessels), but the sum of all these DHW storage losses was only 3 to 4% of the total PE_{use}. Moreover, for 150 L and 200 L vessels, a lower $\dot{m}_{ch}$ reduced the PE_{use} (by up to 11% lower) and the CPP (by up to 22%), though DHW comfort remained at the same level.

In [39], it was concluded that larger, well-insulated storage volumes have a positive effect on the comfort level of end-users with similar PE_{use}, and that $\dot{m}_{ch}$ can be used to optimise energy performance and the CPP of the system. In the following analyses, the $\dot{m}_{ch}$ for the REF-control was always 600 kg/h, and $\%_{PE}$ was always relative to a volume of 90 L.

4.2. Performance Assessment of the TB-Control Strategy

For the TB-control, Figure 6a shows the $t_{DHW;dc}$ and $\%_{PE}$ for 90 L (circle), 150 L (square), 200 L (diamond), and 300 L (star) vessels with $\dot{m}_{ch}$ equal to 600 kg/h. Shorter CTW are indicated by smaller shapes. The REF-control is outlined in black. The TB-control can reduce PE_{use} by up to 60% compared to REF-control, but the DHW discomfort strongly depends on the DHW storage volume and length of CTW. Clearly, 90 L is not sufficient for decentral DHW vessels in case of TB-control, since the smallest $t_{DHW;dc}$ is 9.5% of total tapping time. Larger vessels (200 L and 300 L) have a tipping point where an increase in CTW no longer improves the DHW comfort but only increases PE_{use}. However, note that the PE_{use} of each TB-control variant is always very small compared to the REF-control. The reasons for this increased PE_{use} are twofold. First, Table 2 shows that for 200 L, the distribution losses increase for larger CTWs, due to higher $\%T_{high}$, obviously. However, the $\bar{T}_{ret}$ also increases, which leads to slightly poorer production efficiencies of the GHP (see Equation (4)). This is mainly due to too long of a CTW, so that DHW vessels are fully charged before the CTW ends. In this case, the DHW priority switch is no longer active, and SH is also delivered at a high temperature, as the $T_{sup;SP}$ is still 65 °C. Second,

the temperature sensor is at the bottom of the vessel, so if a resident uses DHW during a CTW, the DHW vessel will be recharged immediately for the second time in that period. This is also reflected in the increased total DHW vessel losses for longer CTW.
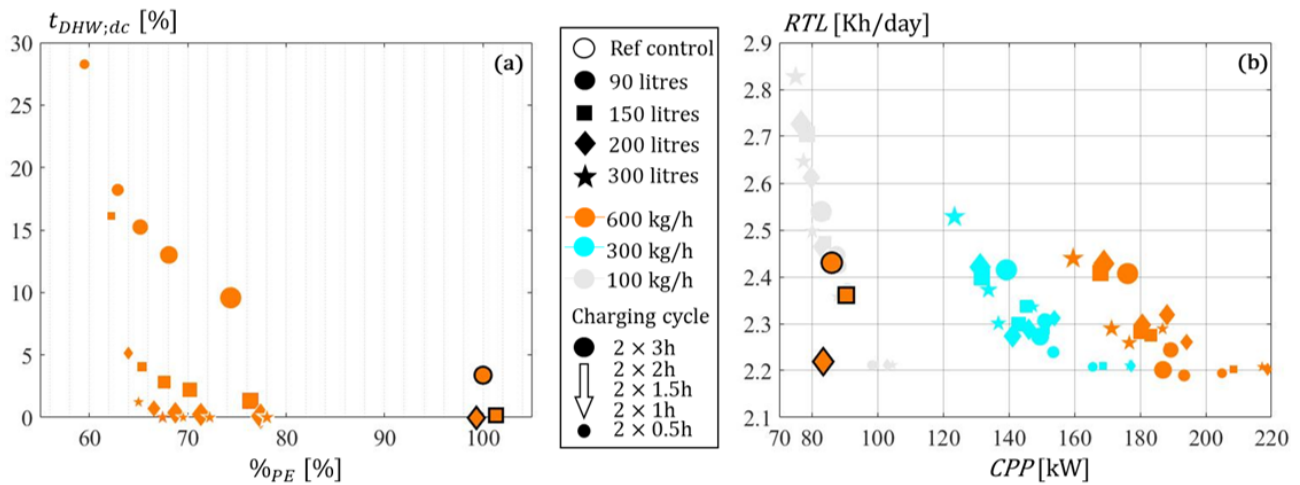

Figure 6. TB-control: (**a**) a Pareto plot of $t_{DHW;dc}$ and $\%_{PE}$ with a $\dot{m}_{ch}$ of 600 kg/h, and (**b**) a Pareto plot of room temperature lack (RTL) and central peak power (CPP). The shape refers to the DHW storage volumes (90 L, 150 L, 200 L, and 300 L). The reference is outlined in black. The $\dot{m}_{ch}$ defines the potential PE savings, but also highly affects the DHW discomfort. The CPP can be reduced to the reference control level by lowering $\dot{m}_{ch}$.

For an $\dot{m}_{ch}$ of 600 kg/h, the time-based grouping results in larger CPP compared to the REF-control (see orange data points in Figure 6b). The CPP even increases for smaller CTWs and smaller DHW vessels (up to 2.5 × the reference CPP of 80 kW). The pre-defined CTWs also affect the RTL. With smaller CTWs, the DHW priority switch is active less often, increasing indoor thermal comfort. This RTL increases slightly (but is still less than 3 Kh/day) when a lower $\dot{m}_{ch}$ is set. However, a smaller $\dot{m}_{ch}$ leads to lower CPP (blue and grey data points in Figure 6b), even to the level of REF-control.

Table 2. Performance of 200 L DHW vessels with increasing CTW. The $\%T_{high}$ and $\bar{T}_{ret}$ increase when the CTW increases, resulting in higher distribution losses. Moreover, the DHW vessels are recharging more often, which also increases the storage losses.

200 L Volume	$\%T_{high}$	$\bar{T}_{ret}$	Distribution Losses	DHW Storage Losses
2 × 0.5 h	4.14%	32.8 °C	392.9 kWh	315.5 kWh
2 × 1 h	8.31%	33.8 °C	410.6 kWh	389.1 kWh
2 × 1.5 h	12.47%	34.9 °C	436.9 kWh	407.5 kWh
2 × 2 h	16.64%	36.0 °C	462.0 kWh	418.9 kWh
2 × 3 h	24.96%	37.6 °C	499.2 kWh	435.5 kWh

A reduction in $\dot{m}_{ch}$ also affects the $t_{DHW;dc}$ and $\%_{PE}$. In general, CTW and volume have the same effect at lower flow rates, as in Figure 6a, but with lower PE_{use} and worse $t_{DHW;dc}$. The tipping point thus shifts towards a larger CTW. The additional energy savings (for 100 kg/h vs. 600 kg/h) are 20% for small CTWs and 8% for larger CTWs and volumes. The increase in $t_{DHW;dc}$ is small for appropriate CTW and volumes. For 300 L vessels, the $t_{DHW;dc}$ of 0% can still be achieved with an $\dot{m}_{ch}$ of 100 kg/h.

4.3. Performance Assessment of the 2SC Strategy

In the 2SC strategy, the central supply temperature is highly dependent on the sensors in the decentralised DHW vessels. Therefore, the positions of the sensors were analysed for 90 L and 150 L vessels, with a $\dot{m}_{ch}$ of 600 kg/h and ±3 °C hysteresis. Afterwards,

the influences of volume, $\dot{m}_{ch}$, and hysteresis were examined with fixed positions for the two sensors.

4.3.1. Sensor Position in Decentralised DHW Vessels

In Figure 7, all possible combinations of the two sensor positions in a 90 L DHW vessel are compared based on (a) $t_{DHW;dc}$ and $\%_{PE}$, and on (b) RTL and $\%T_{high}$. The colours refer to the position of the lower sensor (T1) and the shape to that of the upper sensor (T2). For example, the blue circle for 90 L vessels means that T1 is in the bottom layer (4/5 of the height) and T2 is placed in the second-lowest layer (2/3 of the height). The black star represents the REF-control with 90 L vessels at 600 kg/h and a sensor at 2/3 of the height (the reference). A similar legend is used for 150 L in Figure 7c.

On the one hand, the results show that a higher-positioned T2 saves more primary energy, up to 11.7% compared to the REF-control when T2 is positioned at 1/5 of the height of the vessels (i.e., diamond shape in Figure 7a), but it also causes higher DHW discomfort (smaller "active" volume). The upper sensor initiates the high supply temperature in the CHDC. Therefore, if this sensor is placed higher, the $T_{sup;SP}$ is less likely to be 65 °C, and the PE_{use} will be lower. This reasoning is reinforced by Figure 7b. The $\%T_{high}$ can be reduced to only 43.6% of the time when T2 is in the top layer of the DHW vessels. However, a lower-positioned T2 increases the DHW comfort (smaller $t_{DHW;dc}$) because a larger buffer volume of at least 55 °C (set point of 58 °C–hysteresis of 3 °C) is available, at the expense of increased PE_{use}. The RTL is minimally affected by the position of T2.

On the other hand, $t_{DHW;dc}$ and RTL are mainly influenced by the position of T1. The lower this sensor is placed, the better the DHW comfort, but the worse the indoor thermal comfort, and vice versa. A lower T1 means that a particular DHW vessel is more likely to charge when the central supply temperature is set to 65 °C, and so the charge times of DHW vessels are more grouped, resulting in lower $\%T_{high}$ and $\%_{PE}$. This behaviour of grouped charging results in improved DHW comfort, as earlier recharging ensures that more heat is stored in DHW vessels after DHW consumption. This reduces the chance of DHW discomfort for the next DHW tapping. This earlier recharging of DHW vessels is also the reason for the slightly increased RTL, as there is a priority to provide DHW. When a DHW vessel is recharged, the SH is shut off. However, for any combination of sensor positions, the RTL is low, so the focus is on the trade-off between $\%_{PE}$ and $t_{DHW;dc}$.

The same conclusions can be drawn for 150 and 200 L vessels. In Figure 7c, an extra comparison is made between CPP and PER for 150 L vessels. It can be noted that the top sensor (T2) has a great influence on the CPP and PER, and the bottom sensor (T1) does not affect these KPIs. When T2 is placed higher, the CPP is higher, which is in line with previous findings. Namely, the supply temperature is less likely to be high. Therefore, multiple DHW vessels are more likely to charge simultaneously, causing higher peak demand. In addition, the CPP is always higher than in the REF-control due to the grouping with high $\dot{m}_{ch}$. The higher PER indicates that heat losses are lower than for the REF-control, which is explained in detail in Section 4.3.2.

For the remainder of this research on 2SC, T1 was placed in 90 L vessels at 4/5 of the height and in larger vessels at the second-lowest layer, as this sensor should be as low as possible to minimise $t_{DHW;dc}$ in combination with a low PE_{use}. The upper sensor is placed so that about 30 L of buffer volume is available above T2 to provide a balanced trade-off among $t_{DHW;dc}$, PE_{use}, and CPP.

4.3.2. Other Design Influences on 2SC Strategy

This section compares design variants of 2SC, i.e., different volumes, $\dot{m}_{ch}$, and levels of hysteresis, with the REF-control (at 600 kg/h and hysteresis of 3 °C). The shape refers to the volume (90, 150, or 200 L), the colours to $\dot{m}_{ch}$ (600 to 100 kg/h), and the darkness of a certain colour to the hysteresis (3, 4, or 5 °C). Figure 8 provides Pareto plots for all sensitivity analyses on 2SC, focusing on (a) $t_{DHW;dc}$ and $\%_{PE}$, and on (b) $\%T_{high}$ and CPP.
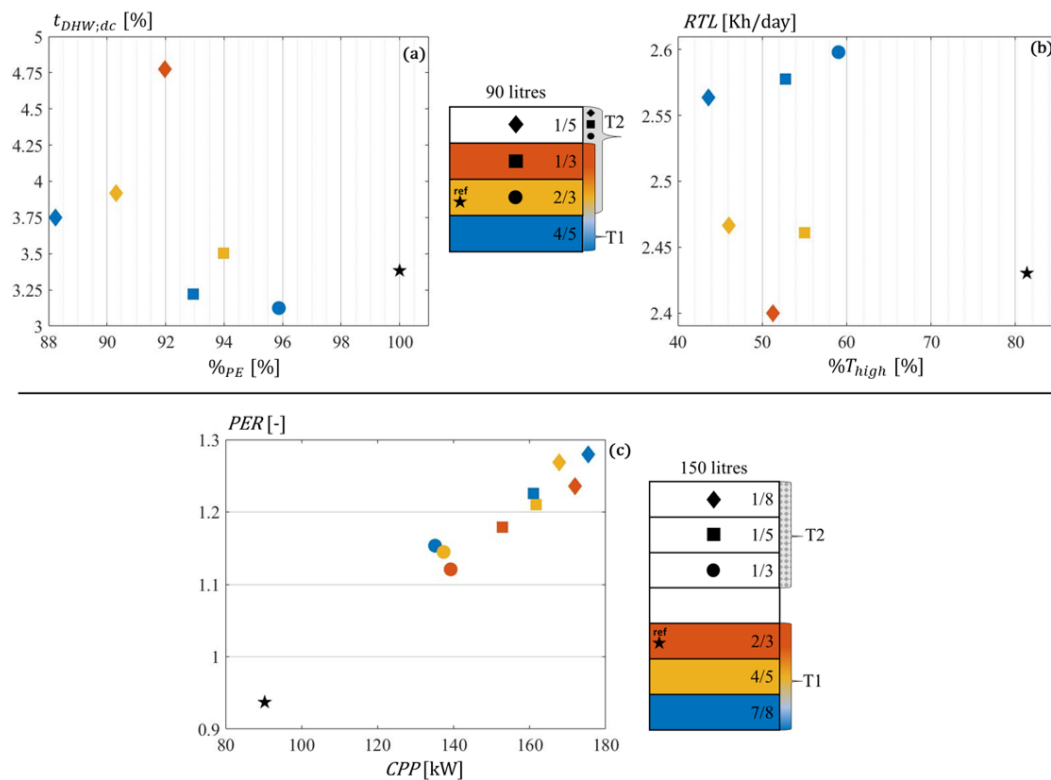
Figure 7. Two-sensor control: Pareto analyses on the sensors' positions in 90 L vessels (**a**) for $t_{DHW;dc}$ and $\%_{PE}$, and (**b**) for RTL and $\%T_{high}$; and in 150 L vessels (**c**) for PER and CPP. The 90 L vessel has four water layers in which place the temperature sensors, and the 150 L one has seven. The colour refers to the place of the lower sensor (T1), and the shape refers to the position of the upper sensor (T2). For example, the blue square for 90 L means that T1 is at 4/5 of the height of the vessel (layer 4), and T2 is to 1/3 of the height (layer 2). The reference is the reference control strategy (600 kg/h charging flow rate) with the sensor placed at 2/3 of the height, for 90 L or 150 L vessels (depending on the graph).

As before, an increase in DHW storage volume reduces $t_{DHW;dc}$, up to 0% discomfort for 200 L DHW vessels. Furthermore, Figure 8a shows that 2SC consumes less PE than REF-control. Increasing the DHW storage volume also increases the potential PE savings, from 5% to 15% for 90 L, to around 25% for 200 L. This is due to better grouping of DHW vessels' recharging. Indeed, see Figure 8b for the 2SC strategy with a $\dot{m}_{ch}$ of 600 kg/h. The $\%T_{high}$ was only 21.5% for 200 L vessels and 52.7% for 90 L, whereas the REF-control had a supply temperature above 50 °C for 81.3% of the time for both volumes. Additionally, the $\bar{T}_{ret}$ was 40 °C for 200 L and 50.3 °C for 90 L in the 2SC strategy. Therefore, the distribution losses are lower and the average COP of the GHP is higher, resulting in better energy performance.

As noted in the TB-control (Section 4.2), the grouping of charging times increased the CPP excessively for large $\dot{m}_{ch}$. However, as Figure 8b suggests, the CPP becomes larger when larger DHW vessels are used. The larger the volume, the longer it takes for the top sensor (T2) in a given DHW vessel to detect a temperature below 58 °C. Therefore, it is more likely that other residents have consumed DHW by the time one of the DHW vessels in the CHDC needs to be recharged. When more vessels are being recharged simultaneously, the CPP increases. Again, reducing the $\dot{m}_{ch}$ has a positive effect on the CPP (for 100 kg/h, the CPP is similar to the reference) and results in a slightly higher $t_{DHW;dc}$. For a hysteresis of 3 °C (light variant of all colours), the PE_{use} and $t_{DHW;dc}$ for all $\dot{m}_{ch}$ are similar for larger vessels. The benefits of a lower $\bar{T}_{ret}$ (reduction of 2.5 °C for $\dot{m}_{ch}$ of 100 kg/h) and the drawbacks of higher $\%T_{high}$ cancel each other out. The heat losses are similar for each

case of 2SC. For 90 L DHW vessels, a smaller $\dot{m}_{ch}$ increases the $t_{DHW;dc}$, as expected, and reduces PE_{use} as $\bar{T}_{ret}$ is reduced by 7.5 °C at 100 kg/h.
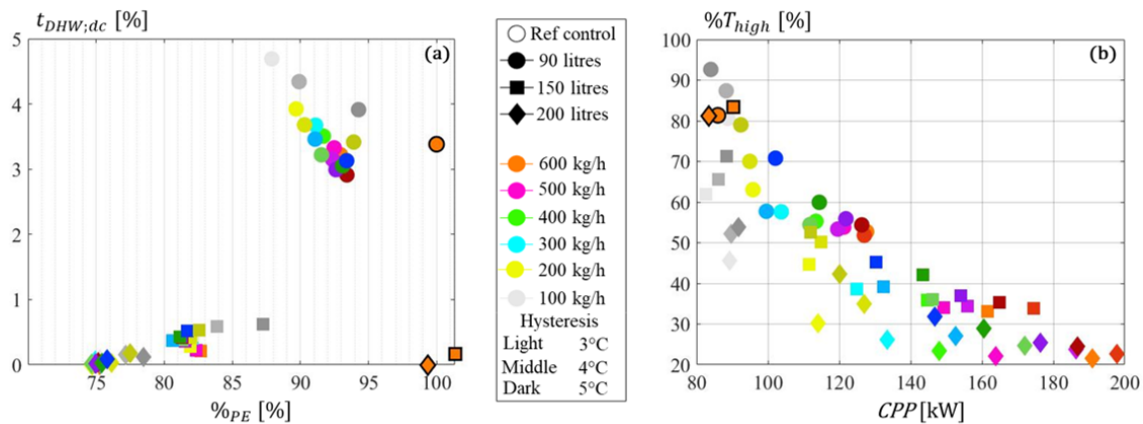

Figure 8. Two-sensor control: Pareto analysis of (**a**) $t_{DHW;dc}$ and $\%_{PE}$, and (**b**) $\%T_{high}$ and CPP for different volumes (different shapes), charging flow rates (different colours), and hysteresis (darkness of certain colour). The REF-control is outlined in black. The 2SC consistently consumes less PE than REF-control, and the $t_{DHW;dc}$ and $\%_{PE}$ are similar for different $\dot{m}_{ch}$ and hysteresis values in the case of large storage volumes. By lowering $\dot{m}_{ch}$, the CPP for the 2SC can be reduced to the level of REF-control.

A larger hysteresis seems to increase the $\%T_{high}$, resulting in higher PE_{use}. However, DHW comfort does not necessarily increase because recharging may start too late (initiated when $T < 58$ °C $-$ hysteresis). For 90 L vessels, the hysteresis has a more pronounced influence and thus can be used to further optimise the charging periods. For all variants of this section, the RTL was between 2.28 and 2.99 Kh/day, with an average of 2.5 Kh/day. The larger the DHW vessel and the larger $\dot{m}_{ch}$, the better the indoor thermal comfort.

4.4. Additional Analyses on Most Representative Variants

In this section, the results of previous analyses are generalised through additional analyses. The $\dot{m}_{ch}$ of reference control was 600 kg/h for each storage volume. For TB-control, all CTWs were considered for 150 L, 200 L, and 300 L. The $\dot{m}_{ch}$ was set to 100 kg/h. This resulted in a similar CPP as for the REF-control, but also slightly higher PE_{use} and $t_{DHW;dc}$, although the CTW and vessel volume were more decisive in this respect. For 2SC, the three representative variants were 90 L with 400 kg/h, and 150 L and 200 L, both with 100 kg/h. The hysteresis was set at ±4 °C for 2SC. The same sensor positions as in Section 4.3.2 were used. In the following graphs, the reference is in black, 2SC variants are in red, and TB-control is in blue.

4.4.1. Number of Dwellings

To investigate the effect of network size, a comparison is made between 6, 10, 20, and 30 dwellings in the apartment building. Figure 9 gives an overview of the results for $t_{DHW;dc}$ and $\%_{PE}$. In smaller apartment buildings, $t_{DHW;dc}$ generally increases for all control strategies. For 2SC, this was up to 5.87% for 90 L vessels at six dwellings. Of course, the CTW length of the TB-control strongly affects $t_{DHW;dc}$, but when a proper CTW length is selected, the $t_{DHW;dc}$ is, e.g., only 2.43% at six dwellings (for two × 3 h and 150 L vessels). As expected, the $\%T_{high}$ is the same for any number of dwellings with TB-control. Additionally, PE savings and $t_{DHW;dc}$ are similar, as only the time settings affect these factors.

Although the network size slightly influences the energy saving potential, the storage volume is generally more decisive on this potential for both the TB-control and the 2SC strategy. For 2SC and 200 L storage, PE savings were 24% at 6 dwellings and 22.31% at 30 dwellings, whereas for 90 L vessels, the savings ranged from 14.81% at 6 dwellings to

only 7.54% at 30 dwellings. For TB-control, the CTW is most important for the potential, and smaller CTWs are possible when larger vessels are used, for all numbers of dwellings.
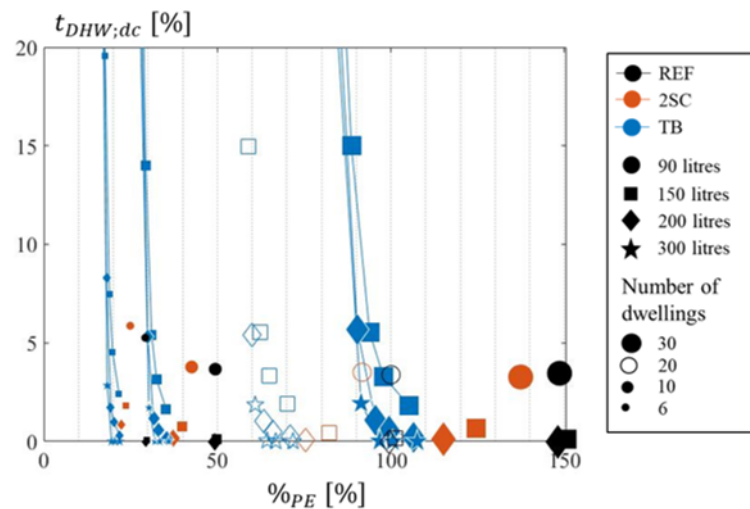

Figure 9. Pareto plot of $t_{DHW;dc}$ and $\%_{PE}$ for a decreasing number of dwellings. The blue data points are for TB-control, red for 2SC, and black for reference control. The size of the data point reflects the number of dwellings (those without a face colour are for 20 dwellings, i.e., the reference situation).

4.4.2. Insulation of Decentralised DHW Vessels

The insulation of decentral DHW vessels was reduced from Ecodesign label "A+" to "C" and to "F". Figure 10 gives two Pareto plots of the results for (a) $t_{DHW;dc}$ and $\%_{PE}$, and (b) RTL and $\%T_{high}$. Obviously, the insulation level influences the PE_{use} for each control strategy, as heat losses increase, and for larger volumes, the relative increase becomes larger. However, the relative increase between "A+" and "F"-labelled DHW vessels was the smallest for TB-control (11.5% and 17% for 150 and 300 L, respectively) and was the largest for 2SC (28% and 48% for 90 and 200 L, respectively). For the REF-control, this increase was 17.6% for 90 L vessels and 23% for 200 L vessels (PE_{use} of 150 and 200 L vessels was about 3.9% greater than for 90 L vessels). Therefore, relative PE savings compared to the REF-control with a given insulation level increased for TB-control and decreased for 2SC. These savings for 2SC ranged from 9.5% ("A+") to 0.35% ("F") for 90 L vessels and from 22.3% ("A+") to 6.6% ("F") for 200 L vessels. For TB-control, these relative savings ranged from 28.6% (200 L, "A+") to 36% (150 L, "F"). The main factor is the increase in $\%T_{high}$. For TB-control, there are predefined CTWs for high temperature; thus, the increase in PE_{use} is only related to more DHW vessels being recharged for longer periods during these time windows. In contrast, the $\%T_{high}$ increased by up to 46% for 2SC. Consequently, the $t_{DHW;dc}$ for each insulation level is similar for 2SC and the reference control, and DHW discomfort increases for smaller vessels and/or smaller CTWs in TB-control.

For each control strategy, the RTL increases due to the priority switch for DHW. Again, the highest increase was found for 2SC, which is related to the highest increase in $\%T_{high}$. Finally, the CPPs for each insulation level are similar for the TB-control and 2SC, but for the REF-control, the range was increased from between 80 and 90 kW to 130 and 140 kW. This large increase for REF-control was due to the high $\dot{m}_{ch}$ of 600 kg/h and the higher probability of having to recharge more DHW vessels at the same time. More recharging cycles are required due to higher thermal losses. In contrast, the TB-control and 2SC have a $\dot{m}_{ch}$ of 100 kg/h, and there the grouping is already built into the control.
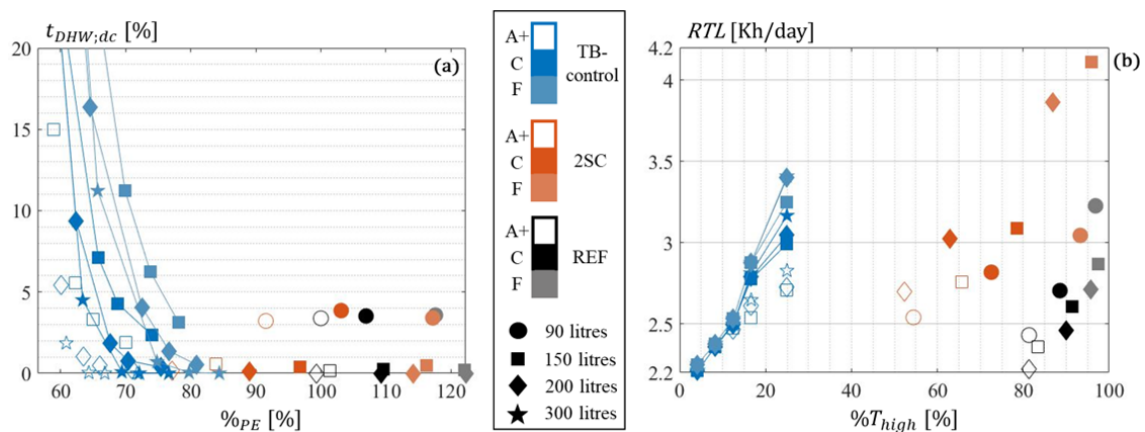
Figure 10. Results for reducing the insulation level of DHW vessels for the three control strategies. The results for $t_{DHW;dc}$ and $\%_{PE}$ are shown in (**a**), and (**b**) shows those for RTL and $\%T_{high}$. The shape refers to the DHW vessel volume, the colour (black, red or blue) to the control strategy, and the greyness of a given colour to the insulation level (white face colour is A+; more grey variant is F).

4.4.3. Electric High-Temperature Unit in the Idealised Central Energy System

In order to generalise the results of this research, different setups of the central energy system were considered. In previous analyses, the high-temperature unit (HT-unit) was a gas boiler, but now the same analyses were performed for an e-boiler or an HT-HP as the central HT-unit. Figure 11 shows $t_{DHW;dc}$ and PER for the three central energy system layouts.
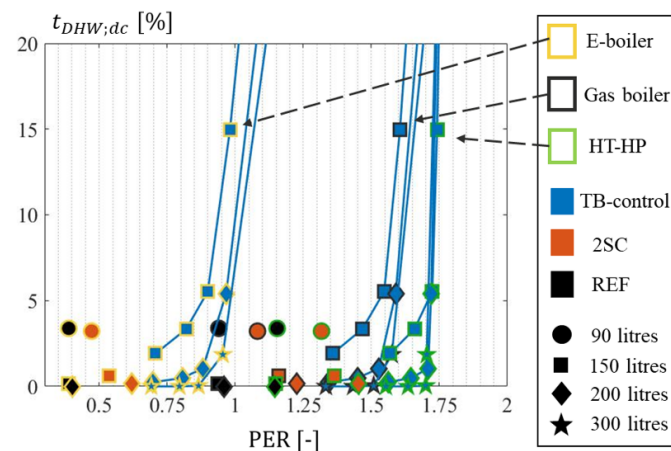

Figure 11. The DHW discomfort and PER for different high-temperature units. The face colour refers to the used control strategy (black for reference control, red for 2SC and blue for TB-control) and the edge colour to the used HT-unit (black is a gas boiler, yellow for the e-boiler, and green for the HT-HP).

Since the central energy system is idealised, end-users' comfort and CPP were the same for all HT-units; only the primary energy consumed, and thus the PER, were different. The different HT-units are clearly visible as groups of data points in Figure 11. On the one hand, the central e-boiler variants (data points outlined in yellow) had the smallest PER, down to only 0.389 for the REF-control. On the other hand, the highest PER was achieved with a central HT-HP (outlined in green)—up to 1.7 with a $t_{DHW;dc}$ below 3.38% of the REF-control. In terms of PE savings, the use of a central e-boiler saved the most—up to 33.9% with 2SC and up to 52.6% with TB-control, compared to the REF-control. Of course, it is assumed that all electricity comes from the Belgian grid, which has an influence on the PE_{use}. The heat production provided by the e-boiler was proportionally greater for the REF-control than for the new temperature-grouping control strategies, and this energy was multiplied by 2.5 to convert to primary energy. With a central HT-HP, the relative PE

savings were smaller (19.2% for 2SC and 31% for TB-control), but the total primary energy consumption was lower, of course, due to better production efficiencies.

4.4.4. Idealised vs. Non-Idealised Central Energy System

In order to validate the results of an idealised central energy system, the performances of the most representative variants were analysed with a non-idealised central energy system, consisting of a GHP and a gas boiler. The results are given in Figure 12. The PE_{use} (see Figure 12a) increased by between 16% and 17% in the case of the non-idealised energy system for the REF-control, between 17% and 19% for the 2SC, and between 16.5% and 18.8% for the TB-control. This means that the relative savings of the non-idealised energy system variants were about 1% less than those previously calculated.
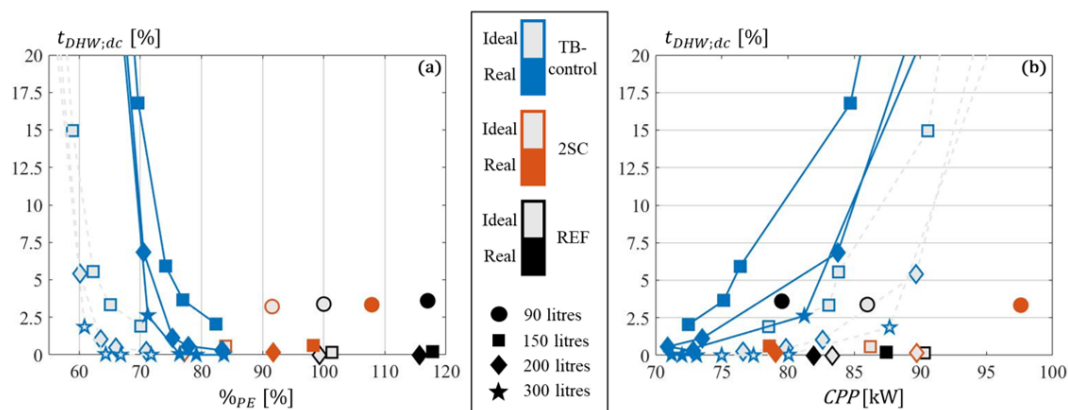

Figure 12. Results for considering a non-idealised central energy system. Graph (**a**) shows the results for $t_{DHW;dc}$ and $\%_{PE}$, and (**b**) for $t_{DHW;dc}$ and CPP. The shape refers to the DHW vessel volume and the colour (black, red, or blue) to the control strategy. An outlined data point is for an ideal central energy system, the other ones are for non-idealised central energy systems.

Figure 12b shows that for a non-idealised energy system, the CPP of each variant decreases compared to an idealised energy system. This is because an idealised energy system is capable of immediately increasing the supply temperature to the desired set point, whereas in a non-idealised energy system, time delays occur due to control and inertia of heat production units. Therefore, the central production units (more specifically, the boiler) cannot deliver the demanded temperature instantaneously, and this results in a lower CPP.

The presence of time delays in the non-idealised energy system do not lead to a significant increase in $t_{DHW;dc}$. As with the ideal energy system, $t_{DHW;dc}$ is mainly influenced by the size of the DHW vessels, and for TB-control, the duration of the CTW. Therefore, the sizing of the central energy system was adequate for the examined variants, and it can be stated that the conclusions of this research with an idealised energy system are valid for realistic cases.

5. Discussion

The work [56] argues that advanced control strategies are needed to unlock the flexibility of district heating and cooling, or collective heating in general, with respect to smart energy systems (i.e., including the electricity grid). While this is true, the current research shows that large energy savings are already possible within the thermal network itself by using this flexibility in a smart way. The presented methodology to group the demands for low-temperature and high-temperature leads to significant PE savings, up to 36%, in a CHDC with decentralised DHW vessels, while still delivering the thermal comfort to end-users. Aside from designing new control strategies to reduce the supply temperature, the limitations should also be identified, as stated by [57], to enhance the transition towards low-temperature networks. Therefore, the main limitations and potentials are discussed here for the two control strategies that group the demands of similar temperature levels.

First, the TB-control requires larger storage volumes (at least 150 L in the case of DHW storage) to bridge periods of low supply temperature. By reducing $\dot{m}_{ch}$ to 100 kg/h, the CPP can be reduced to the level of the REF-control. This means that the size of central production units can remain as before by grouping high-temperature demand vessels, and it even lowers the PE_{use}. In contrast, this lower $\dot{m}_{ch}$ slightly increases the $t_{DHW;dc}$. The effects of CTW length are most important for maintaining DHW comfort and lowering PE_{use}. These time settings are also highly dependent on the DHW consumption pattern of inhabitants and need to be optimised for each building. In general, there is a tipping point where increasing the CTW does not improve DHW comfort but only increases PE_{use}, and this tipping point is reached faster with larger vessels.

Second, the 2SC always results in PE savings while maintaining DHW comfort. However, the $t_{DHW;dc}$ might be higher when the sensors are not optimally positioned. The lower sensor (T1) should be as low as possible to minimise $t_{DHW;dc}$ in combination with a low PE_{use}. This has a small effect on end-user comfort and CPP. The effect of low positions on the temperature sensors' accuracy needs to be checked with real measurements. For the upper sensor (T2), a trade-off exists among $t_{DHW;dc}$, PE_{use}, and the CPP. A higher position leads to lower DHW comfort and higher peak demand, but results in larger energy savings. In the case of decentralised DHW vessels, around 30 L needs to be available above the sensor to secure DHW comfort, which is in line with findings of [45]. Again, a smaller $\dot{m}_{ch}$ lowers the CPP, while still providing DHW comfort and still saving PE compared to REF-control. For only 90 L vessels, $\dot{m}_{ch}$ cannot be lower than 400 kg/h, as the $t_{DHW;dc}$ becomes much larger than for the REF-control at 600 kg/h. The hysteresis does not affect performance too much but can be used for minor optimisations when the storage volumes exceed 90 L.

Moreover, the effects of the concept's boundary conditions on the performance of control strategies were investigated. First, the number of dwellings does not affect the performance of TB-control significantly, but for the 2SC, the energy savings increase and DHW comfort decreases for smaller dwellings. The main reason for poorer DHW comfort is the lower probability of a given upper sensor detecting a temperature that is too low ($<58\,^\circ$C $-$ hysteresis). Therefore, the DHW vessels are less likely to pre-charge based on the low-priority temperature sensor, since the central supply temperature is less likely to be high. On the contrary, larger networks are in favour of the TB-control (when the CTW and decentralised storage are large enough). The same goes for reduced vessel insulation rates. When the vessels have an "F"-labelled insulation, the heat losses increase, certainly for larger storage tanks where the highest PE savings are realised, resulting in higher $\%T_{high}$. Therefore, the advantage of being able to group the high-temperature recharging is partly lost, as there are far too many standing losses to compensate for. In this respect, the 2SC can only achieve minor savings (up to a maximum of 6.6% for 200 L vessels). Finally, it is shown that grouping high-temperature demands save energy in different types of energy systems and are useful for electrification. When less sensible choices are made for the selection of the HT-unit, such as an e-boiler, the relative savings are higher, but the total energy use is also the largest (as was also stated in [30]). Obviously, better HT-unit design choices, such as fully HP-based central energy systems, lead to the lowest PE_{use}.

The conclusions of this research can be extended to large-scale DH. There, decentralised storage vessels are deployed for better integration of HP and to increase the system's flexibility [57]. The vessels might also be used to store heat for different space heating systems and insulation levels of different neighbourhoods, where also other temperature levels are required in the different parts of the network and/or during times of the day. When the size of the CHDC is increased to 50 or 100 dwellings for the 2SC and there is a high-temperature HP as the HT-unit, the potential savings at range from 4.9% (90 L) to 18.14% (200 L) 50 dwellings and from 1.68% (90 L) to 18% (200 L) for 100 dwellings. For small storages, the potential depends heavily on the number of dwellings for the 2SC. It is suggested to use larger storage vessels in large buildings to maximise the probability of grouped charging. In fact, Jansen et al. [58] recently developed a model predictive controller

to optimise the supply temperature in a low-temperature DH, resulting in energy savings of 3% to 17%. The control strategy also lowered the supply temperature when no large heat demand was expected in the near future and thus exploited the thermal inertia of the building. However, this control strategy did not consider the DHW production through the central production units, as decentralised booster heat pumps were used, and the case consisted of 12 similar dwellings; thus, the temperature differences were not as large as in the current research.

The sizing of the non-idealised central energy system led to a similar performance and similar savings as in the idealised centralised energy system. Moreover, the sizing method validated in [54] can be used for the examined concept to size the central heat production. However, it currently uses the standard DIN4708 [59] to determine the heat demand for DHW. This standard calculates the total heat demand based on instantaneous DHW demand, and therefore does not take into account the effects of decentral DHW vessels and $\dot{m}_{ch}$ on the peak heat demand. As a consequence, the physical or theoretical meaning behind the standard is lost. As shown in this study, the volume, the $\dot{m}_{ch}$, and the control strategy affect the peak demand; therefore, to be compatible with the used sizing method, further research is required to translate the effects of these influences into appropriate design guidelines.

Other future research questions for optimising the grouping of same-temperature-level requirements for collective heating systems with decentralised vessels are as follows:

- Using data-oriented techniques to further optimise the grouping method. The findings in this paper will help in developing data-oriented controllers for CHDC with decentral DHW vessels, as the optimisation opportunities and shortcomings have been investigated, and the estimated 35.8% PE savings of Section 2.2 have not been reached for 90 L vessels with good DHW comfort. Two main points of attention are to control the $\dot{m}_{ch}$ more appropriately (e.g., variable $\dot{m}_{ch}$ based on the DHW demands and CPP) and achieve larger savings in the case of a poor DHW vessel insulation rate and small storage volumes.
- Including space cooling in a CHDC with decentralised DHW vessels. Until now, this has not been considered possible for this heating concept, as a high temperature is always needed. However, grouped control offers opportunities for space cooling, since the %T_{high} can easily be reduced to less than 40% of the day. The difficulty, however, is that space cooling is not possible when the supply temperature is too high, and vice versa. Therefore, the main concern is the number of temperature changes, as this affects exergy losses, but too-few switches lead to thermal discomfort in dwellings.

6. Conclusions

The supply temperature is of great importance for the performance of an HP-based system, but different temperature levels are required for end-users. However, state-of-the-art supply-temperature-control strategies do not focus on grouping the same-temperature demand to allow different temperature throughout the day. Rather, they focus on reducing the return temperature or flow rate while keeping the supply temperatures the same throughout the day. Only decentralised booster heat pumps are considered valid to reduce the supply temperature, but they lead to more refrigerant in the system and usually investment costs that are too high [15]. Therefore, this research presented a new supply temperature control method that groups the high-temperature and low-temperature demand in a 2-pipe collective heating system.

In this respect, decentralised DHW vessels in CHDC can store the DHW locally and provide the flexibility needed to switch between high and low supply temperatures. The method is assessed by means of two new rule-based control strategies. First, a time-based control strategy where the supply temperature level is predetermined by time slots. Here, two charging time windows were predefined to increase the temperature to 65 °C to recharge all decentralised DHW vessels. These two CTWs start on average 30 min before the largest increase in DHW demand of the entire apartment building. Second, we presented

a new sensor-based control approach where two sensors are used in each decentralised DHW vessel. Controlling the supply temperature based on those sensors, rather than time of day, makes the control strategy generalisable and less case-dependent. The presented control strategies can be a benchmark for other control strategies, e.g., data-oriented ones.

Furthermore, the impact and optimisation limits of concept and design choices on performance have been identified. The assessment framework is based on dynamic simulation in which the main KPIs were end-user thermal comfort, primary energy consumption, and central peak power. Based on this evaluation, the following main conclusions are drawn.

- Optimisation potential of grouping same-temperature demands:
    1. For well-insulated storage vessels, a larger volume increases the DHW comfort without negatively affecting the PE_{use} for each control strategy used. In fact, higher potential savings were found for larger storage volumes.
    2. The TB-control led to the highest potential savings, up to 36%. However, time settings related to these CTWs are very case-specific and need to be optimised for each heating network. These energy savings are the same as those initially estimated, but with at least 150 L of storage volume to provide sufficient DHW comfort.
    3. The 2SC strategy guarantees DHW comfort in every case with PE savings of up to 27%. Only for 90 L vessels might the $t_{DHW;dc}$ exceed 5%. Smaller collective heating networks enable higher savings, but with poorer DHW comfort, due to the lower probability of low-priority charging. In large networks (50+ dwellings), the savings potential is only 1–7% with 90 L vessels; therefore, larger volumes are recommended to increase the potential to 20%.
    4. The $\%T_{high}$ was between 8.5% and 25% for TB-control, taking into account DHW comfort, and obviously depends only on the time settings. For 2SC, it could vary between 15% and 95%, and this is mainly influenced by the insulation level (A+ insulation yields the highest energy savings and lowest $\%T_{high}$) and $\dot{m}_{ch}$ (a higher flow rate lowers the $\%T_{high}$, but increases the CPP). This enables potential for space cooling in CHDCs.
- Limiting factors for grouping same-temperature demands:
    1. The $\dot{m}_{ch}$ should be low to reduce the CPP to the level of the REF-control. This slightly decreases the potential PE savings, but still provides thermal comfort to end-users. Thus, central production units and distribution pipes do not necessarily need to be larger.
    2. TB-control requires larger storage vessels, and 2SC is possible with small, well-insulated vessels in smaller networks, but for larger networks, larger vessels are advised.
    3. With TB-control, a smaller CTW results in higher PE savings, but at the expense of DHW comfort. A tipping point for CTW lengths can be identified for each volume and $\dot{m}_{ch}$, where a larger CTW only results in more PE_{use} for similar DHW comfort.
    4. The PE savings of 2SC are highly dependent on the insulation level of the DHW vessels, but 2SC always ensures DHW comfort. Savings are only 6.5% with "F"-labelled insulation. Moreover, the positions of the two sensors can be used to optimise the performance. In the case of DHW vessels, the upper sensor provides end-users comfort, and about 30 L should be available as a buffer volume above this sensor. The position of the lower sensor should be as low as possible.

Data Availability Statement: The data presented in this study are available on request from the corresponding author. The data are not publicly available because they are part of ongoing research.

Conflicts of Interest: The authors declare no conflict of interest.

Nomenclature

2SC	Two-Sensor Control strategy
$\%_{PE}$	Relative Primary Energy savings [%]
$\%T_{high}$	Time Percentage of High $T_{sup;SP}$ [%]
CHDC	Combined Heat Distribution Circuit
CHE	Coil Heat Exchanger
COP	Coefficient of Performance
c_p	Specific Heat Capacity [J/kgK]
CPP	Central Peak Power [kW]
C	Thermal Capacity [J/K]
CTW	Charging Time Window
DH	District Heating
DHW	Domestic Hot Water
e-boiler	Electric Boiler
$f_{CHE;vol}$	CorrectiOn Factor for Sizing the Internal CHE of DHW Vessels
(G)HP	(Geothermal) Heat Pump
HT-HP	High-Temperature Heat Pump
HT-unit	High-Temperature unit
KPI	Key Performance Indicator
$\dot{m}$	Mass Flow Rate [kg/s]
$\dot{m}_{ch}$	Charging Flow Rate of Decentralised DHW vessels [kg/s]
$n_{v;tot}$	Total Ventilation Rate [h^{-1}]
PE_{use}	Primary Energy use [kWh]
$\dot{Q}$	Heat Flux of Component [W]
P_{boi}	Fossil Fuel Use of Boiler [kWh]
P_{HP}	Electricity Use of HP [kWh]
r	Radiation Share of Heat Flux [%]
r_i	Radius of Pipe at Place i [m]
REF-control	Reference Control strategy
RTL	Room Temperature Lack [Kh/day]
SH	Space Heating
TB-control	Time-Based Control Strategy
$t_{DHW;dc}$	Duration of DHW Temperature Lack Relative to Total Tap Time [%]
T	Temperature [°C]
$\bar{T}_{ret}$	Average Return Temperature Of CHDC [°C]
$T_{sup;SP}$	Supply Temperature Set Point [°C]
UA	Overall Heat Transfer Coefficient [W/K]
V	Volume [m³]
Greek letters	
Δt	Simulation Time Step [s]
λ	Conductivity of a Material [W/m²K]
ρ	Mass Density [kg/m³]
τ	Time Constant of Valves (32 s)

Subscripts	
em	emitter
ext	exterior/outdoor
in	inlet
int	internal
out	outlet
prd	production unit
sol	solar
v	ventilation
w	wall
z	zone (indoor air and furniture)

References

1. European Commission and Directorate-General for Climate Action. *Going Climate-Neutral by 2050: A Strategic Long-Term Vision for a Prosperous, Modern, Competitive and Climate-Neutral EU Economy*; Publications Office: Luxemburg, 2019. [CrossRef]
2. Mathiesen, B.; Bertelsen, N.; Schneider, N.; García, L.; Paardekooper, S.; Thellufsen, J.; Djørup, S. *Towards a Decarbonised Heating and Cooling Sector in Europe: Unlocking the Potential of Energy Efficiency and District Energy*; Aalborg Universitet: Aalborg, Denmark, 2019.
3. Lund, H.; Möller, B.; Mathiesen, B.V.; Dyrelund, A. The role of district heating in future renewable energy systems. *J. Energy* **2010**, *35*, 1381–1390. [CrossRef]
4. Paardekooper, S.; Lund, R.; Mathiesen, B.; Chang, M.; Petersen, U.; Grundahl, L.; David, A.; Dahlbæk, J.; Kapetanakis, I.; Lund, H.; et al. *Heat Roadmap Belgium: Quantifying the Impact of Low-Carbon Heating and Cooling Roadmaps*; Aalborg Universitet: Aalborg, Denmark, 2018.
5. Persson, U.; Wiechers, E.; Möller, B.; Werner, S. Heat Roadmap Europe: Heat distribution costs. *Energy* **2019**, *176*, 604–622. [CrossRef]
6. Lund, H.; Werner, S.; Wiltshire, R.; Svendsen, S.; Thorsen, J.E.; Hvelplund, F.; Mathiesen, B.V. 4th Generation District Heating (4GDH): Integrating smart thermal grids into future sustainable energy systems. *Energy* **2014**, *68*, 1–11. [CrossRef]
7. De Pauw, M.; Van Riet, F.; De Schutter, J.; Binnemans, S.; Van der Veken, J.; Verhaert, I. A methodology to compare collective heating systems with individual heating systems in buildings. In Proceedings of the REHVA Annual Meeting Conference: Low Carbon Technologies in HVAC, Brussels, Belgium, 23 April 2018.
8. Lund, H.; Duic, N.; Østergaard, P.A.; Mathiesen, B.V. Future district heating systems and technologies: On the role of smart energy systems and 4th generation district heating. *Energy* **2018**, *165*, 614–619. [CrossRef]
9. Sayegh, M.; Jadwiszczak, P.; Axcell, B.; Niemierka, E.; Bryś, K.; Jouhara, H. Heat pump placement, connection and operational modes in European district heating. *Energy Build.* **2018**, *166*, 122–144. [CrossRef]
10. Vering, C.; Maier, L.; Breuer, K.; Krützfeldt, H.; Streblow, R.; Müller, D. Evaluating heat pump system design methods towards a sustainable heat supply in residential buildings. *Appl. Energy* **2022**, *308*, 118204. [CrossRef]
11. Ghane, S.; Jacobs, S.; Casteels, W.; Brembilla, C.; Mercelis, S.; Latré, S.; Verhaert, I.; Hellinckx, P. Supply temperature control of a heating network with reinforcement learning. In Proceedings of the 2021 IEEE International Smart Cities Conference (ISC2), Manchester, UK, 7–10 September 2021; pp. 1–7. [CrossRef]
12. Jacobs, S.; Van Riet, F.; Verhaert, I. A collective heat and cold distribution system with decentralized booster heat pumps: A sizing study. In Proceedings of the Building Simulation 2021: 17th Conference of IBPSA, Bruges, Belgium, 1–3 September 2021; Volume 17, pp. 223–230. [CrossRef]
13. Rasheduzzaman, M.; Singh, R.; Haas, C.N.; Gurian, P.L. Required water temperature in hotel plumbing to control Legionella growth. *Water Res.* **2020**, *182*, 115943. [CrossRef] [PubMed]
14. Zhu, T.; Ommen, T.; Meesenburg, W.; Thorsen, J.E.; Elmegaard, B. Steady state behavior of a booster heat pump for hot water supply in ultra-low temperature district heating network. *J. Energy* **2021**, *237*, 121528. [CrossRef]
15. Østergaard, P.A.; Andersen, A.N. Economic feasibility of booster heat pumps in heat pump-based district heating systems. *J. Energy* **2018**, *155*, 921–929. [CrossRef]
16. Vaillant Rebollar, J.E.; Himpe, E.; Laverge, J.; Janssens, A. Sensitivity analysis of heat losses in collective heat distribution systems using an improved method of EPBD calculations. *Energy* **2017**, *140*, 850–860. [CrossRef]
17. Yang, X.; Pan, L.; Guan, W.; Tian, Z.; Wang, J.; Zhang, C. Optimization of the configuration and flexible operation of the pipe-embedded floor heating with low-temperature district heating. *Energy Build.* **2022**, *269*, 112245. [CrossRef]
18. Yang, X.; Li, H.; Svendsen, S. Energy, economy and exergy evaluations of the solutions for supplying domestic hot water from low-temperature district heating in Denmark. *Energy Convers. Manag.* **2016**, *122*, 142–152. [CrossRef]
19. Meireles, I.; Sousa, V.; Bleys, B.; Poncelet, B. Domestic hot water consumption pattern: Relation with total water consumption and air temperature. *Renew. Sustain. Energy Rev.* **2022**, *157*, 112035. [CrossRef]
20. Fuentes, E.; Arce, L.; Salom, J. A review of domestic hot water consumption profiles for application in systems and buildings energy performance analysis. *Renew. Sustain. Energy Rev.* **2018**, *81*, 1530–1547. [CrossRef]

21. Fang, X.; Gong, G.; Li, G.; Chun, L.; Peng, P.; Li, W.; Shi, X.; Chen, X. Deep reinforcement learning optimal control strategy for temperature setpoint real-time reset in multi-zone building HVAC system. *Appl. Therm. Eng.* **2022**, *212*, 118552. [CrossRef]
22. Su, B.; Wang, S. An agent-based distributed real-time optimal control strategy for building HVAC systems for applications in the context of future IoT-based smart sensor networks. *Appl. Energy* **2020**, *274*, 115322. [CrossRef]
23. Sun, Y.; Li, X.; Wei, W.; Xue, H.; Wang, W.; Deng, S. Development of a variable water temperature control method for air source heat pump based on the supply–demand balance. *Sustain. Energy Technol. Assess.* **2022**, *52*, 102366. [CrossRef]
24. Sun, Y.; Chen, X.; Wu, S.; Wei, W.; Wang, W.; Deng, S. Performance analysis of air source heat pump space heating system with an adaptive control for supply water temperature. *Appl. Therm. Eng.* **2022**, *211*, 118401. [CrossRef]
25. Verhelst, C.; Logist, F.; Van Impe, J.; Helsen, L. Study of the optimal control problem formulation for modulating air-to-water heat pumps connected to a residential floor heating system. *Energy Build.* **2012**, *45*, 43–53. [CrossRef]
26. Luc, K.M.; Li, R.; Xu, L.; Nielsen, T.R.; Hensen, J.L. Energy flexibility potential of a small district connected to a district heating system. *Energy Build.* **2020**, *225*, 110074. [CrossRef]
27. Benakopoulos, T.; Vergo, W.; Tunzi, M.; Salenbien, R.; Svendsen, S. Overview of Solutions for the Low-Temperature Operation of Domestic Hot-Water Systems with a Circulation Loop. *Energies* **2021**, *14*, 3350. [CrossRef]
28. Vaillant Rebollar, J.E.; Himpe, E.; Laverge, J.; Janssens, A. Influence of recirculation strategies in collective distribution system on the performance of dwelling heating substations. In Proceedings of the VIII International Conference for Renewable Energy, Energy Saving and Energy, Havana, Cuba, 25–28 May 2015; pp. 1–10.
29. Cholewa, T.; Siuta-Olcha, A.; Anasiewicz, R. On the possibilities to increase energy efficiency of domestic hot water preparation systems in existing buildings—Long term field research. *J. Clean. Prod.* **2019**, *217*, 194–203. [CrossRef]
30. Dermentzis, G.; Magni, M.; Ochs, F.; Monteleone, W.; Schaffer, B. Heat Pump Solutions in Renovations of Multi-Storey Buildings. In Proceedings of the CLIMA 2022 Conference: The 14th REHVA HVAC World Congress, Rotterdam, The Netherlands, 22–25 May 2022. [CrossRef]
31. Vanhoudt, D.; Claessens, B.; Salenbien, R.; Desmedt, J. An active control strategy for district heating networks and the effect of different thermal energy storage configurations. *Energy Build.* **2018**, *158*, 1317–1327. [CrossRef]
32. Huang, T.; Yang, X.; Svendsen, S. Multi-mode control method for the existing domestic hot water storage tanks with district heating supply. *Energy* **2020**, *191*, 116517. [CrossRef]
33. Yang, X.; Svendsen, S. Improving the district heating operation by innovative layout and control strategy of the hot water storage tank. *Energy Build.* **2020**, *224*, 110273. [CrossRef]
34. Stalinski, D.; Duquette, J. Development of a simplified method for optimally sizing hot water storage tanks subject to short-term intermittent charge/discharge cycles. *J. Energy Storage* **2021**, *37*, 102463. [CrossRef]
35. Verhaert, I.; Bleys, B.; Binnemans, S.; Janssen, E. A Methodology to Design Domestic Hot Water Production Systems Based on Tap Patterns. In Proceedings of the CLIMA 2016 Conference: REHVA 12th HVAC World Congress, Aalborg, Denmark, 22–25 May 2016.
36. Lyu, W.; Wang, Z.; Li, X.; Deng, G.; Xu, Z.; Li, H.; Yang, Y.; Zhan, B.; Zhao, M. Influence of the water tank size and air source heat pump size on the energy saving potential of the energy storage heating system. *Energy Storage* **2022**, *55*, 105542. [CrossRef]
37. Efkarpidis, N.A.; Vomva, S.A.; Christoforidis, G.C.; Papagiannis, G.K. Optimal day-to-day scheduling of multiple energy assets in residential buildings equipped with variable-speed heat pumps. *Appl. Energy* **2022**, *312*, 118702. [CrossRef]
38. Vandermeulen, A.; van der Heijde, B.; Patteeuw, D.; Vanhoudt, D.; Helsen, L. A theoretical benchmark for bypass controllers in a residential district heating network. *Energy* **2018**, *151*, 45–53. [CrossRef]
39. Jacobs, S.; De Pauw, M.; Hellinckx, P.; Verhaert, I. Decentralized storage in combined heat distribution circuits: How to control? In Proceedings of the CLIMA 2022 Conference: The 14th REHVA HVAC World Congress, Rotterdam, The Netherlands, 22–25 May 2022. [CrossRef]
40. KMI. Algemeen Klimaat België. Available online: https://www.meteo.be/nl/unpublish/algemeen-klimaat-belgie/maand-per-maand/januari/ (accessed on 23 April 2022). (In Dutch)
41. Kayfeci, M.; Yabanova, İ.; Keçebaş, A. The use of artificial neural network to evaluate insulation thickness and life cycle costs: Pipe insulation application. *Appl. Therm. Eng.* **2014**, *63*, 370–378. [CrossRef]
42. Vlaams Energie—en Klimaatagentschap. Bijlage V—Bepalingsmethode EPW 2022. Available online: https://www.energiesparen.be/bouwen-en-verbouwen/epb-pedia/epb-regelgeving/energiebesluit/bijlage-v/ (accessed on 9 February 2022). (In Dutch)
43. Van Riet, F. Hydronic Design of Hybrid Thermal Production Systems in Buildings. Ph.D Thesis, University of Antwerp, Antwerpen, Belgium, 2019.
44. Jorissen, F.; Reynders, G.; Baetens, R.; Picard, D.; Saelens, D.; Helsen, L. Implementation and verification of the IDEAS building energy simulation library. *J. Build. Perform. Simul.* **2018**, *11*, 669–688. [CrossRef]
45. VLAIO. Productie en Distributie van Sanitair Warm Water: Selectie en Dimensionering. 2012–2014. TETRA 120145. Availabel online: https://www.tetra-sww.be/ (accessed on 9 February 2021). (In Dutch)
46. VLAIO. Instal 2020 project: Integraal Ontwerp van Installaties Voor Sanitair en Verwarming. 2014–2018. VIS 135098. Availabel online: https://www.instal2020.be/ (accessed on 9 February 2021). (In Dutch)
47. Klein, S.A.; Duffie, J.A.; Mithell, J.C.; Kummer, J.P.; Thornton, J.W.; Bradley, D.E.; Arias, D.A.; Beckman, W.A.; Duffieet, N.A.; Braun, J.E.; et al. Mathematical Reference: Type 54 (Hourly Weather Data Generator). In *TRNSYS 17*; Energy Laboratory University, University of Wisconsin-Madison: Madison, WI, USA, 2009; Volume 4, pp. 303–306.

48. Klein, S.A.; Duffie, J.A.; Mithell, J.C.; Kummer, J.P.; Thornton, J.W.; Bradley, D.E.; Arias, D.A.; Beckman, W.A.; Duffieet, N.A.; Braun, J.E.; et al. Mathematical Reference: Type 60 (Stratified fluid storage tank with internal heat exchangers). In *TRNSYS 17*; Energy Laboratory University, University of Wisconsin-Madison: Madison, WI, USA, 2009; Volume 4, pp. 390–396.
49. ClimaWays BVBA. Collindi Verwarmingssatellieten: Geïndividualiseerde Collectieve Verwarmingssystemen. Datasheet. Available online: https://docplayer.nl/12558563-Geindividualiseerde-collectieve-verwarmingssystemen-geintegreerde-sturing-met-energiekostenverdeling.html (accessed on 13 September 2021). (In Dutch)
50. Van Riet, F.; Janssen, E.; Steenackers, G.; Verhaert, I. Hydronic design of cogeneration in collective residential heating systems: State-of-the-art, comparison and improvements. *Appl. Therm. Eng.* **2019**, *148*, 1246–1257. [CrossRef]
51. Van Riet, F.; Steenackers, G.; Verhaert, I. A new approach to model transport delay in branched pipes. In Proceedings of the 10th International Conference on System Simulation in Buildings, Liege, Belgium, 10–12 December 2018.
52. Viessmann. Planningsaanwijzing Vitocal 300-G. Datasheet. 5818 541 B/fl, Vitocal 350-G type BW 351.B24. 2016; p. 47. Available online: https://www.manualslib.com/products/Viessmann-Vitocal-350-G-Bw-351-B42-10942119.html (accessed on 13 September 2021). (In Dutch)
53. Verhaert, I. Design methodology for combined production and distribution for domestic hot water and space heating. In Proceedings of the CLIMA 2019 Conference: REHVA 13th HVAC World Congress, Bucharest, Romania, 26–29 May 2019, pp. 1–7. [CrossRef]
54. Van Minnebruggen, S.; Verhaert, I. In-situ validation of a new sizing methodology for combined production and distribution for domestic hot water and space heating. In Proceedings of the Building Simulation 2021: 17th Conference of IBPSA, Bruges, Belgium, 1–3 September 2021; Volume 17, pp. 2989–2996. [CrossRef]
55. *Standard ISO 52000-1:2017*; Energy Performance of Buildings—Overarching EPB Assessment—Part 1: General Framework and Procedures. ISO: Geneva, Switzerland, 2017.
56. Vandermeulen, A.; van der Heijde, B.; Helsen, L. Controlling district heating and cooling networks to unlock flexibility: A review. *Energy* **2018**, *151*, 103–115. [CrossRef]
57. Guelpa, E.; Capone, M.; Sciacovelli, A.; Vasset, N.; Baviere, R.; Verda, V. Reduction of supply temperature in existing district heating: A review of strategies and implementations. *Energy* **2023**, *262*, 125363. [CrossRef]
58. Jansen, J.; Jorissen, F.; Helsen, L. Optimal control of a fourth generation district heating network using an integrated non-linear model predictive controller. *Appl. Therm. Eng.* **2023**, *223*, 120030. [CrossRef]
59. *Standard DIN4708-2*; Central Heat-Water-Installations—Part 2: Rules for the Determination of the Water-Heat-Demand in Dwelling Houses. Deutsches Institut für Normung: Berlin, Germany, 1994.